Locating Regulating Resources in the WECC to Damp Electromechanical Oscillations

A Thesis Presented for the

Master of Science

Degree

The University of Tennessee, Knoxville

Michael John Breuhl

May 2018

Acknowledgments

I thank my family and friends for their help throughout my college career. I would like to thank my parents Kevin Gleason, Jennifer Gleason, Jonathan Breuhl, and Mabel Breuhl for their support throughout my college career. I would like to especially thank Dr. Hector Pulgar for his guidance, patience, and assistance throughout my research and studies. I want to thank my fellow graduate student Horacio Silva for his help throughout my research experience with his insight and guidance. I want to thank the rest of the research team: Yajun Wang, Mojtaba Jalalpour, and Jonathan Devadason with their support as well. I want to thank the CURENT, the Center for Ultra-Wide-Area Resilient Electric Energy Transmission Networks, professors Dr. Kevin Tomsovic, Dr. Kai Sun, Dr. Fran Li, and Dr. Yilu Liu with their assistance through my coursework and group meetings that have helped shape not only my research, but also my understanding of power systems. I also want to say thank you to CURENT for allowing me the opportunity to study power system and renewables since my undergraduate program until now.

Abstract

As we gradually move towards higher penetration of renewable energy sources, the grid must have a safe, feasible, and stable operation at each penetration level. For any penetration level throughout this transition, what is a way to identify and install regulation resources such as energy storage devices to effectively damp critical oscillations? Power system planners lack a simple criterion on how to deploy regulation resources and must rely on heavy calculations such as modal analysis or Prony analysis. This thesis hypothesizes that no matter how complicated the oscillations' behavior and interactions can be, in the case of critical inter-area oscillations, the location to install regulating resources are more importantly related to the system physical characteristics rather than operational characteristics. The focus of this thesis is on the system distribution of inertia in the Western Electricity Coordinating Council (WECC). This goal of this study is to analyze the impact of wind power on the inter-area oscillations WECC system, determine the locations for potential regulation resources, and identify key critical areas for higher wind penetrations.

From the analysis of the WECC system, only a few key areas related to machines participating in a given oscillation are viable for a significant improvement through regulation resources. These machines are generally machines in the weaker inertia group of generators. At higher renewable penetrations the machines in the east, southeast, and southwest see higher residue sensitivity index (RSI) values, which means that these areas are more susceptible to active power injections and oscillations in the WECC. The changes in the system with the wind turbine generators (WTGs) highly impact the RSI values, which is due to the topology changes in the system. The RSI does not change significantly for different stable operation points of the system.

Table of Contents

List of Tables

List of Figures

Chapter 1

Introduction

1.1 Motivation

Due to changing standards and regulations towards clean energy sources in the US, power systems are shifting towards higher penetrations of renewable energy (RE) sources. The current Western Interconnection (WI) has approximately 5% wind energy and 2% solar energy in net generation, but the WI is conducting studies to increase this percentage [2]. This can be seen from reports such as *Western Wind and Solar Integration Study*, which studies the implementation of 35% of renewable energy sources by 2017 for the WECC system [1]. There are many aspects concerning the power grid that can be studied, but two key issues are the variability for renewable sources such as solar and wind energy and the lack of inertia for normal wind turbine generators. These issues are properly addressed in order to ensure the stability of the WI for the current RE penetration. As the renewable penetration increases, there will be an effect on the stability of the system. This can be seen with the electromechanical dynamics for a given multi-machine system which is defined in Equation (1.1).

$$2H\frac{\mathrm{d}f(t)}{\mathrm{d}t} = \Delta P \tag{1.1}$$

In Equation 1.1, H is the equivalent system inertia constant given in seconds, f(t) is the equivalent system frequency in p.u., and ΔP is the change in power for a given disturbance in p.u. [3]. This equation shows that for a system that decommissions synchronous generators, the system will have a lower overall inertia and leads to a high ROCOF. With the loss of synchronous generators there is a reduction in the relative inertia of the power system and an increase of variability in generation. Ulbig, Borsche, and Andersson show that the reduction in rotational inertia decreases the stability of the system during an imbalance between the generation and the load, which will cause frequency deviations, an exchange of transient power, and faster frequency dynamics [4]. The current worldwide goals of incorporating renewables into power grid has brought about literature to ensure stable operation. Not only does the load demand of the system need to be supplied, but also the grid also need to be resilient to faults, maintain grid frequency, and reliably transfer power. A few examples of this literature is the effects of converter based generation on power system modes and operation, exploration into wide area control methods, frequency control with renewable sources, and allocation of regulating devices.

1.2 State of the Art

One aspect concerning high renewables in the power grid that has been studied is how power grids will change with the addition of renewable energy through converter-based sources. There is a shift in the use of wind turbines from fixed-speed wind turbines and variable-slip turbines that allow a wider range of control to more converter-based sources such as the doubly-fed induction generator (DFIG) and fully rated wind turbines that allow for better power extraction and control [5]. With the change towards more converter based wind control there have been studies on the impact on the power system mode oscillations with an increase in renewable penetration. One such study had looked into the impact on path flows, displacement of synchronous machines, and the interaction of converter control-based generators (CCBG) with damping torque for the system of the Western Electricity Coordinating Council (WECC). The analysis focused on the participation of the CCBG where they had found that CCBG state variables had low participation in the traditional inter-area electromechanical modes, but could impact the observability of such modes [6]. The study had found that the change in frequency response of the system is not due to the performance of the CCBG pertaining to the operation conditions in the study, but more with the changes in the transmission, generation, and load [6]. Lastly, there were new oscillatory mode types that appeared where the first was exclusively due to the CCBG and the second was an interaction between the CCBG and SG control loops [6].

In order to improve and assure reliable grid operation, many studies are focused on the implementation of energy storage systems. One particular study looks at the optimal placement and sizing of the energy storage using a loss sensitivity index with respect to the battery energy storage systems (BESS) control parameters [7]. Once the optimal location is identified, the study then uses particle swarm optimization in order to identify the optimal energy capacity and power capacity of the BESS [7]. The study had found that with an optimal location, the system had seen a 10.35% increase in the reduction of losses as well as a 24.76% reduction in voltage violations. For the various scenarios with differing wind generation and load levels, the BESS reduced the losses in the system even when the BESS was in charging mode [7]. Along with increasing the reliability of power grids through energy storage, there has been research related to use the RE sources such as solar and wind farms to aid in frequency regulation. In order to aid frequency regulation, the RE generation sites use synthetic inertia and governor controls to make the system more robust. One study using the Eastern Interconnection (EI) and the Texas Interconnection looks at using synthetic inertia to give the system time for other controls to react to faults in the grid [8]. When the frequency control is implemented in the renewable generation sources, there was an improvement in the ROCOF, but a decrease in the nadir [8]. The nadir is the minimal point the frequency will reach during a frequency excursion. The study finds that the inertia control values can be tuned through simple methods related both the generation desired and the average inertia in the system. This way the overall system inertia will not be impacted negatively with more renewable generation sources [8]. This study gives ideas on how future power grids can be affected by renewable integration. Another method of analysis to aid in the understanding of increasing RE penetrations is from a study looking into the placement of energy storage systems to help dampen the critical oscillation in the Northern Chile Interconnected System [9]. By using residue-based eigenvalue sensitivity in the Northern Chile Interconnected System (NCIS), a sensitivity map was developed for the oscillation of the NCIS against the Argentinian Interconnected System (AIS). By inspection, the farther away the regulating resources are from the center of inertia, the higher the impact. An estimate of the system inertia distribution and a high correlation has been found with the sensitivity index of the figure. The speculation from this work is that with a simple decision criterion merely based on the system distribution of inertia, the deployment of BES in the NCIS would have provided useful regulation to damp the critical inter-system oscillation (around 0.5%) [9].

For future grids with high RE penetration, many countries will be reliant upon wind energy. This is great for times of peak wind for maximum power extraction, but in cases of low wind some wind farms are unable to provide power and frequency regulation during faults. One method proposed to help with this phenomena is to use an allocation method with wide-area damping controllers (WADCs) using modal-based control allocation [10]. This method distributes the control signals to active actuators based upon the modal system in order to assure system operation. The study had tested the method with various faults in the WECC system and found sufficient damping and resilience [10].

1.3 Literature Review

1.3.1 Modal Analysis

In order to identify the modes under study, we must perform the methods of modal analysis. This involves linearization of a system as shown in Equations (1.2) and (1.3), which show how state variables of the system will react to small perturbations [11].

$$\dot{x} = Ax + Bu \tag{1.2}$$

$$y = Cx + Du \tag{1.3}$$

$\dot{x}$ refers to *nx1* of the derivative of the state variables, x is *nx1* the state variable matrix, u is the *mxn* input matrix, y is the *nx1* output matrix, A is the system matrix, B is the input matrix, C is the output matrix, and D is the feedforward matrix [11]. Solving Equations

(1.4), (1.5), (1.6) to find the eigenvalues, right eigenvector, and left eigenvector.

$$(A - \lambda I)\,\Phi = 0 \tag{1.4}$$

$$A\Phi_i = \lambda_i \Phi_i \tag{1.5}$$

$$\Psi_i A = \lambda_i \Psi_i \tag{1.6}$$

λ is the eigenvalues of the system, Φ is the solution to the Equation (1.4) for a given eigenvalue, Φ_i is the right eigenvector, and Ψ_i is the left eigenvector [11]. With the left and right eigenvectors we can use the participation factors in order to identify which state variables have a high participation for a given eigenvalue. With equation (1.4), the eigenvalues are calculated and the stability of the system is verified with Lyapunov's first method. Lyapunov's first method gives an estimate of the stability of the non-linear system based upon the eigenvalues of the linearized system. This is evaluated where if the eigenvalues have real parts that are negative, then the system is asymptotically stable [11]. Given that each eigenvalue is an oscillatory mode within the power system and that the power system is stable, the critical inter-area modes can then be identified.

For a given power system, there are local modes and inter-area modes. Local modes are referring to machines at a given station swinging against the rest of the system. Inter-area modes are referring to a group of machines oscillating against another group of machines at different locations in the system [11]. The analysis performed takes into consideration the inter-area modes which are low-frequency modes that can potentially increase the wear and tear on generator hardware. The inter-area modes studied involve a damping ratio (DR) of 10% or less, which is defined by equation (1.7).

$$\zeta = \frac{-\alpha}{\sqrt{\alpha^2 + \beta^2}} \tag{1.7}$$

ζ is the damping ratio, α is the real part of λ_i, and β is the imaginary part of λ_i [12].

1.3.2 Residue Analysis

Previously mentioned in the state of the art section was a study using a residue sensitivity analysis concerning the critical oscillation between the NCIS and the AIS. This analysis method is going to be used in our study to help identify potential areas that require additional active and reactive power injection. This residue index is defined by Equation (1.7) which relates the ability of a regulation device, in our case an energy storage system, to damp a given oscillation [13] [14].

$$\left|\frac{\partial \lambda_\alpha}{\partial K}\right| = \left|\omega_\alpha^T \frac{\partial A_\alpha}{\partial K} v_\alpha\right| = |R_\alpha| \left|F\left(\lambda_\alpha\right)\right| \tag{1.8}$$

λ_α is the given oscillation under study, K is the gain of the controller, ω_α^T is the left eigenvector, A_α is the system matrix , v_α is the right eigenvector, R_α is the residue value, and $F\left(\lambda_\alpha\right)$ is the transfer function to represent the regulation device. The residue value gives an indicator of how effective the controller will be for a given location and is defined as $R_\alpha = C_\alpha v_\alpha w_\alpha^T B_\alpha$. In the study, the residue has been shown to have an implicit relationship with the inertia of a system [13].

1.4 Objectives

1.4.1 General Objective

Due to the transition of power systems moving towards a higher penetration of RE, the goal of this study is to see how a power system will change at varying levels of wind penetration. The test case used in the study is the 181-bus model of the WECC system [15][16]. The evolution in wind penetration is expected to be gradual and, therefore, during this transition (at each penetration level), the system stability must be guaranteed for a feasible and safe operation. Then, in any given penetration level within this transition, which locations to install regulating resources such as Energy Storage (ES) would be more effective to damp oscillations? From a planning perspective, which locations of new RE projects are going to impact more critically the dynamic performance of the power system? In order to give an idea of potential locations and understand how the system will change, the residue sensitivity analysis explained in Equation (1.2) will be applied to the WECC system.

Rather than a unique critical oscillation, the WECC system has three inter-area modes and multiple low damped modes. As a result, the analysis of this system will be multi-dimensional considering these three oscillations as goals and the distribution of inertia of these three areas as parameters. The correlation of the inertia distribution and the oscillation damping improvement will be evaluated. This will be further tested under several operating conditions (a strong criteria would weakly depend on operating conditions) and several scenarios of RE penetration and decommissioned schedules of conventional power plants.

1.4.2 Specific Objectives

- Identify the inertia distribution of the WECC for a base case and its evolution for increasing penetration of renewable energy and decommission schedules of conventional power plants
- Analyze the effect of system operation on the inertia distribution
- Provide guidelines for locating regulating resources based on inertia regions that need to be supported by these devices under different levels of renewable penetration and several scenarios for the decommission of conventional power plants
- Test the results in the Large Scale Testbed (LTB) WECC system for different locations of regulating resources in the WECC and under different fault/event conditions

1.5 Thesis Organization

The thesis is organized in the following format. Chapter 2 concerns the background information of the WECC system and analysis of the base scenario of the WECC system. Chapter 3 concerns the background and analysis of primary frequency controllers with wind turbine generators of the wind scenarios and their impact towards inter-area oscillations. Chapter 4 concerns the application of energy storage to the WECC system. Chapter 5 concludes the contributions and presents the future work.

Chapter 2

WECC Test Cases

2.1 Test System

The test system used for our analysis is the WECC summer test case that is represented by Figure 2.1 [15] [16]. The model was adapted to be used in the power system software DIgSILENT PowerFactory. The generator model is the standard round rotor model which includes the effects of the field winding and additional damping windings for the direct axis and quadrature axis [17]. An interesting characteristic is there are areas in the system with high voltages which may reach up to 1.159 p.u. after contingencies. The highest inertia area is the north, which is an equivalent representation of the northern area of the real WECC system and the highest power concentrations are related to the northern, eastern, and southwestern areas shown in Figure 2.2, which represent the geographic locations of the buses based upon phasor measurement unit locations in the WECC system. The largest inertia machines are located in northern most part representing the equivalent area of British Columbia. The total system inertia values range from 4.294 seconds (s) to 500 s for a given system base of 100 Mega Volt-Amperes (MVA).

2.1.1 Wind Scenarios

In order to get an idea of how the WECC will evolve with wind, there is a need to develop scenarios in order to test different possibilities of the future power grids. Each of the scenarios

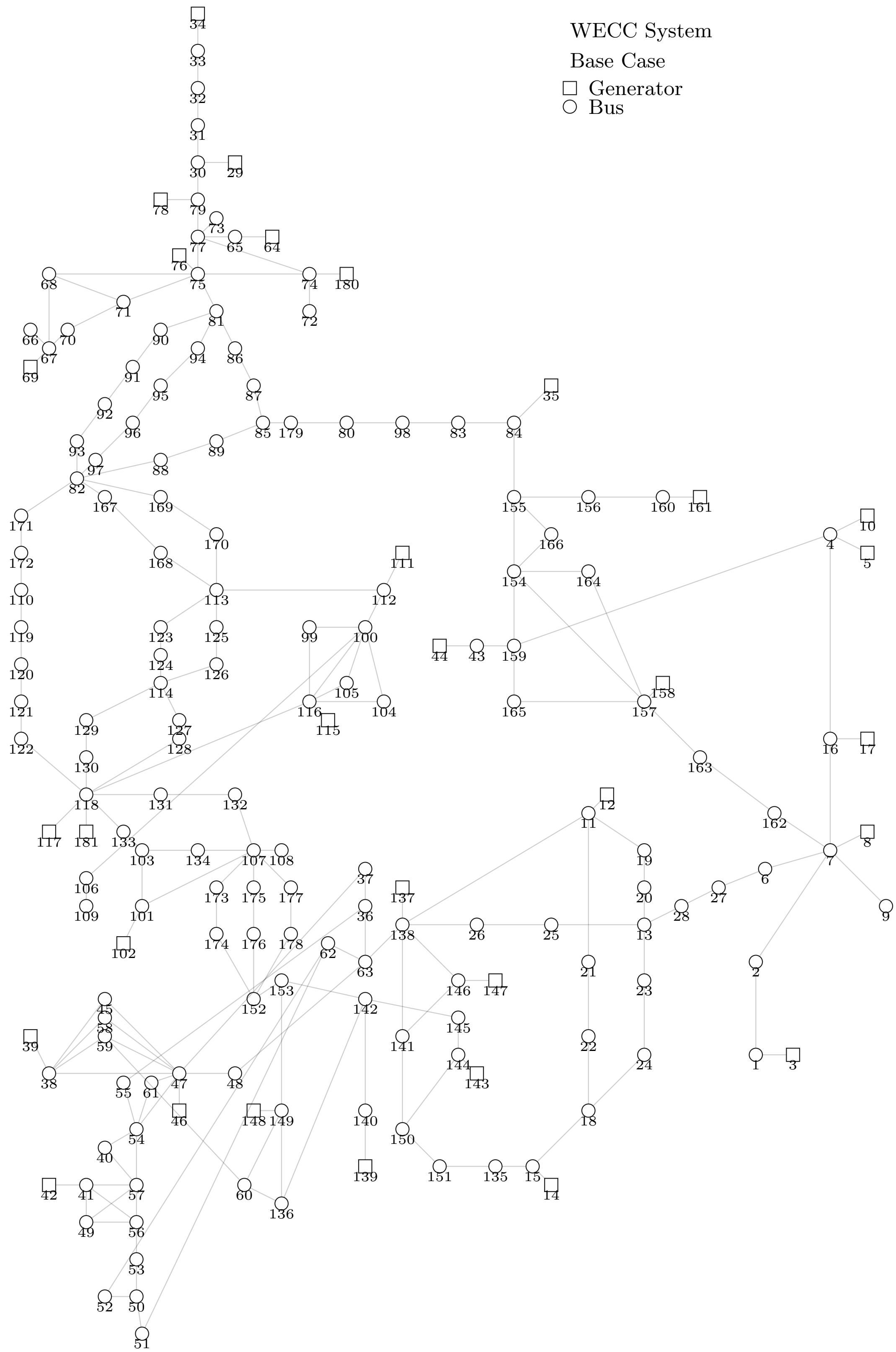

Figure 2.1: WECC Test System

has an extra wind site due to the limits on the power paths and generation capacity of the wind sites from Scenarios 5 and 6.

2.1.2 Background on oscillations of the WECC

Bulk power systems deal with critical oscillations related to synchronous generators during disturbances due to the exchange of energy involved. In the WECC system, the critical inter-area modes are the North-South mode A, North-South mode B, East-West mode A, East-West mode B, British Columbia mode, and the Montana mode [18]. North-South mode A and B are related to the British Columbia and Alberta tie-line; mode A has damping typically between 10% to 15% depending on the strength of the tie-line and loading throughout the day and mode B has a damping value dependent on the loading of the system anywhere between 5% to 10% [18][19]. The East-West mode A has damping around 10% to 13% and East-West mode B is around 11% to 12% based upon Prony and modal analysis performed on the 2015 Heavy Summer and 2022 Light Spring WECC models [20]. The British Columbia mode is the Northwest oscillating against the British Columbia area and the Montana mode is the Montana area oscillating against the Northwest [18]. The analysis that follows uses the knowledge of these six modes and is aimed towards identifying how the WECC may change with increased renewable penetration levels in regards to inertia, changes in the electromechanical modes, and impact of regulation devices.

2.1.3 Analysis

In order to first understand how the WECC will change with wind, a base case without any wind power is analyzed. The application of the residue sensitivity index (RSI) is applied to understand the peak location points for regulation devices. In linear theory, a way to improve a system is to look at the controllability matrix Φ and observability matrix Ψ from Equation (1.5) and Equation (1.6) where $\Psi = \Phi^{-1}$ [11]. By using the controllability matrix to determine the mode controllability, which can be shown as $B' = \Phi * B$. The B matrix can be used to determine what input to change for improvement in system dynamic behavior [11]. In this case, the system operator will not be able to always observe the changes seen

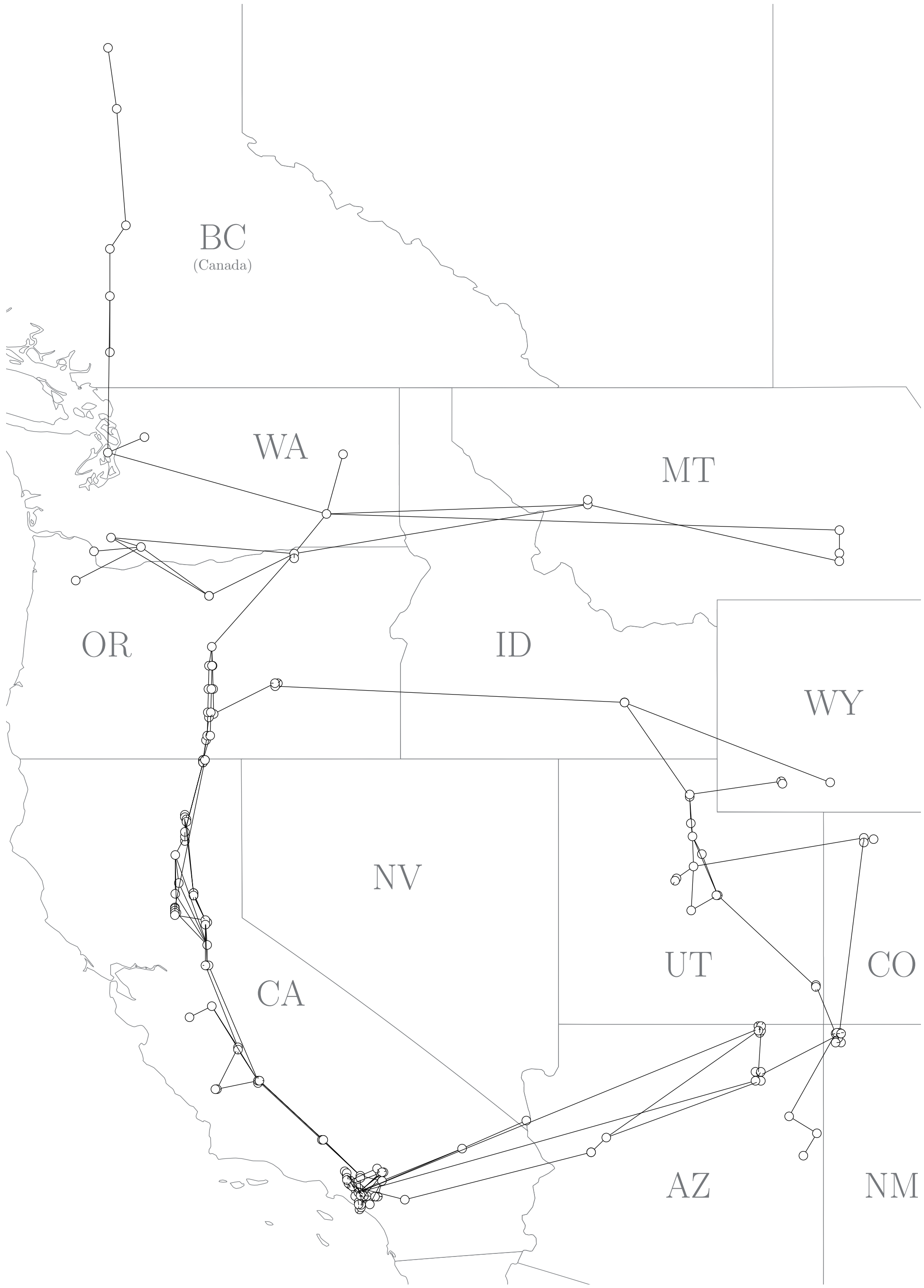

Figure 2.2: WECC Geographic Diagram

Table 2.1: Renewable energy potential for each state defined by rated power (MW) [1]

State	30% Rating Wind Power (MW)
Arizona	11,200
Colorado East	11,589
Colorado West	900
New Mexico	2,790
Nevada	7,050
Wyoming	2,340
California-Oregon Border	180
Idaho East	780
Idaho Southwest	1,500
Montana	1,050
Norther California	11,790
Southern California	14,490
Northwest	12,930
Utah	2,730

Table 2.2: Wind scenarios defined by wind penetration level, scenario type, and wind farm locations

Scenario Number	Wind Penetration	Scenario Type	Wind Farm Locations
1	0% Wind	Base Case	N/A
2	10% Wind	Decommission	2, 4, 7, 16
3	20% Wind	Decommission	2, 4, 7, 16, 138, 144, 146, 149
4	30% Wind	Decommission	2, 4, 7, 16, 68, 77, 138, 144, 146, 149
5	10% Wind	Scale	1, 11, 47, 67, 74, 84, 116, 118, 156
6	20% Wind	Scale	1, 11, 47, 67, 74, 83, 116, 118, 156
7	30% Wind	Scale	1, 11, 47, 67, 74, 83, 116, 118, 140, 146, 156, 171

in the eigenvalue plot of the system. The residue sensitivity analysis is used to gain the best locations of regulation devices that give the greatest impact on both controllability and observability [13]. This gives a system operator or researcher the ability to see how the eigenvalues will change given a regulation device and whether the device has an improvement to the damping of the system. Prior work on the residue analysis index was proven to have a significant impact on the Chilean system's critical inter-area mode with a damping ratio of around 0.5% [9].This showed promise and will be applied towards the WECC system. In this study, the focus will be on the impact towards inter-area oscillations concerning the WECC system.

The regulation device to test the given following residue map is a battery energy storage system (BESS). The BESS has a set of voltage, frequency, active power, and reactive power measurements. The controllers used are a PQ-controller, charge controller, converter, and a battery model [21]. The frequency controller compares the frequency difference to determine the change in the required power. And then the PQ controller is used to help change the current values in order to determine the desired active power (P) and reactive power (Q) output into the charge controller. The charge controller keeps track of the current state of charge and limits the change in voltage and currents in order to not damage the device [21]. The limited currents are then transformed through the converter to give the desired P and Q values to respond only in the event of a disturbance. The BESS does not inject P or Q during normal system operation.

In order to study the effect of the regulation device and RSI, the critical modes are studied. One such mode has a DR of 9.730% which is shown in Figure 2.4. Figure 2.4 shows the RSI plot of the mode with DR 9.730% and the mode shape of the oscillation regarding this mode. The mode shape was determined by implementing a PLL at every bus in the system. The residue map shows key areas for regulation devices sensitive to active power injection and the oscillation map shows the two groups oscillating against one another. The oscillation map shows that between groups there are no jumps in the angles, there are clear distinctions between the oscillating groups. From the residue map the highest potential point is bus 10 for the mode with damping ratio of 9.730%. The residue index is validated through time domain simulations, where we excite the mode through increasing generator 10's speed

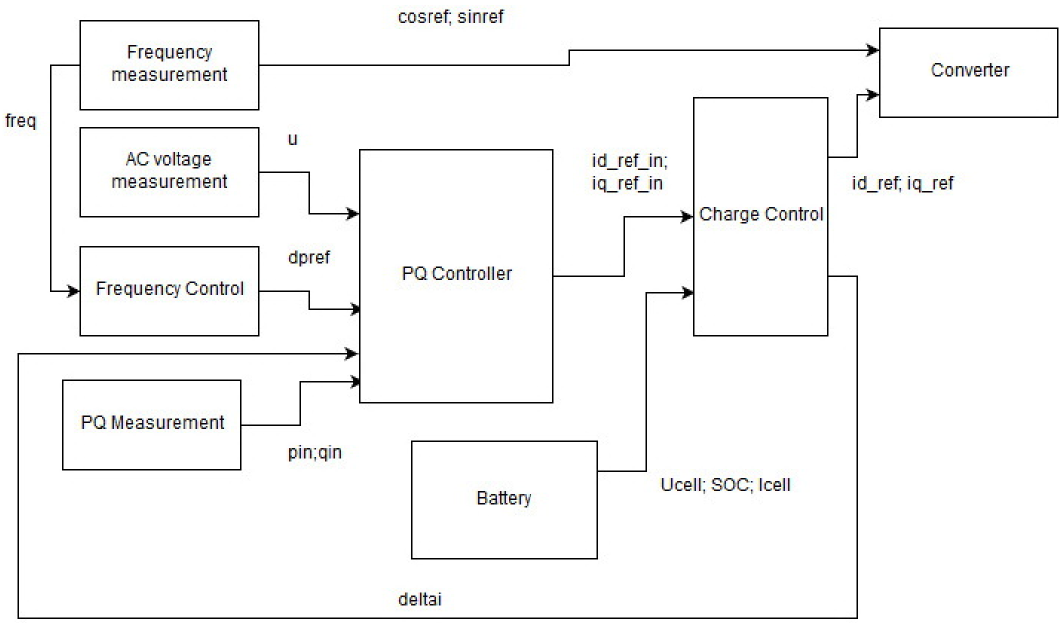

Figure 2.3: Battery Energy Storage Control Diagram

from 1 per unit to 1.02 per unit shown in Figure 2.5. Generator 10 was chosen because the chosen mode has the highest participation factor related to the speed of the machine. In Figure 2.6, the speed of generator 10 (left) and the speed of generator 139 (right) is shown with the three cases of no battery, a battery in the highest potential area, and a battery in a medium potential area, which is bus 159. Figure 2.5 shows that with proper placement the oscillation can be damped within 5 seconds to close to a speed of 1 p.u. An improper placement of the BESS device causes the oscillations to increase in magnitude and frequency.

To verify that the map works with other disturbances in the grid, a short circuit is performed from line bus 7 to bus 16. The placement for BESS is the same as the generator speed event. In Figure 2.5, the speeds for generator 10 and generator 139 are shown. There is an improvement in damping of the magnitude for both generator 10 and 139. The magnitude of the oscillation is much smaller, but these simulations show that the residue has an impact on the inter-area oscillations in the systems.

There are many critical modes with a damping ratio less than 10% in the WECC system, which includes both intra-area and inter-area modes. Table 2.3 summarizes the critical inter-area modes for the WECC system. Due to the ring shape of the WECC system there is an effect where the oscillating generator groups are not completely two large groups. There are always two large areas oscillating against one another, but in some modes a single, large inertia generator can oscillate with a group of generators. In terms of the RSI, when there is a significant difference in the inertia between the oscillation groups, then the maximum RSI will occur in the area of lower inertia. An example of the oscillating groups is shown in Figure 2.4, which shows one group of machine oscillating in blue against another group of machines in red. When the inertia of the two oscillating groups are close together in this system, approximately $0 < H < 60$, then the maximum RSI can occur in the area of higher inertia. The specific example is Mode 6, where the inertia of generator groups are $H_{G1} = 1030$ and $H_{G2} = 970$. The RSI becomes higher with higher damping ratio modes, where the inertia of the groups of machines involved have a lower overall inertia compared to the machines involved in the three lower damped modes. From the residue data in Table 2.3, there are repeated areas that have the highest inertia in multiple modes. In Figure 2.1, there are three areas that are repeated throughout all the inter-area and intra-area modes. The machines participating in these oscillations are generators: 111, 115, 117, 139, 44, 158, 161, and 35. These machines are referring to Northern California (111, 115, 117), Utah (44, 158, 161, 35), and Southern California (139) shown by the clusters of buses in the geographic diagram of the WECC system in Figure 2.2. The Southern California region is a high load area due to the high population with many generation sources, but the high potential area denoted by the RSI is related specifically generator 139. Generator 139 is the highest inertia machine by approximately 3 to 70 times the other inertia values within Southern California. Due to this being the largest inertia generator in the south, this machines ends up with a high participation factor in critical oscillations that other generators oscillate against. Northern California is a long distance from the other generation sites in the ring shape of the WECC system and only has a handful of generators in the region. These generators have lower inertia values where there is an imbalance between generation and loading and must import generation from the Northern US and British Columbia. This contributes to the high residue potentials at generators 111 and 115 since the machines have less inertia and generation compared to the load in the area. Utah is a high cluster of generation and loading in the eastern part of the WECC system. This low inertia area is connected to the other

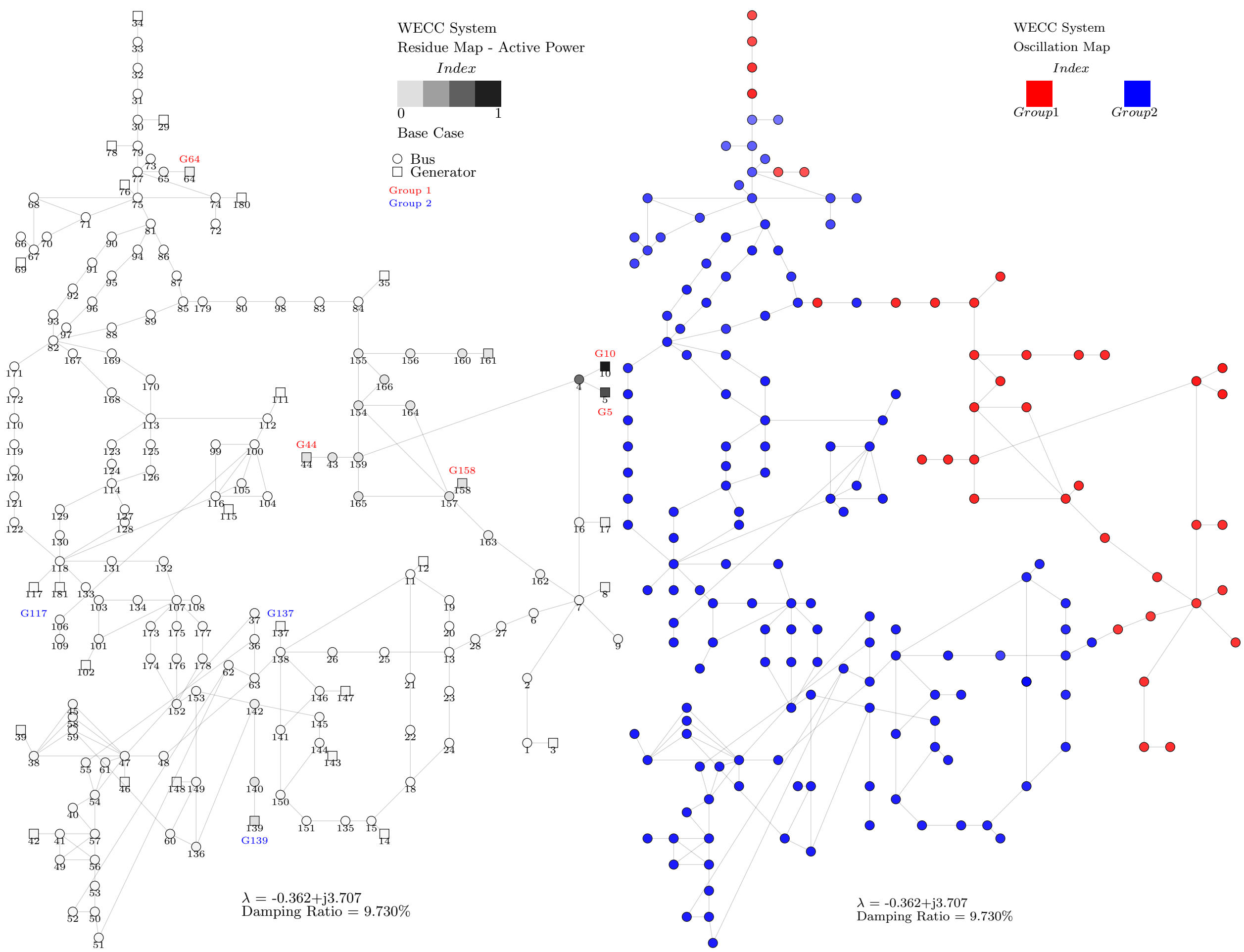

(a) Residue Map **(b)** Oscillation Map

Figure 2.4: (a) Residue map and (b) Mode shape for the inter-area mode with DR 9.730%

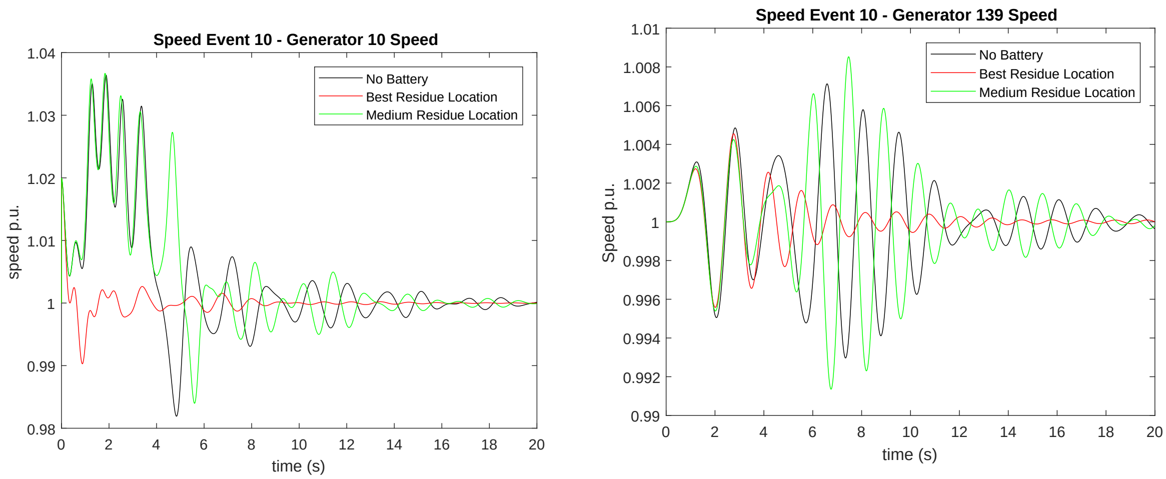

(a) Generator 10

(b) Generator 139

Figure 2.5: Generator 10 speed event for mode with DR 9.730%. Simulations show speed for (a) Generator 10 and (b) Generator 139 for various energy storage system locations

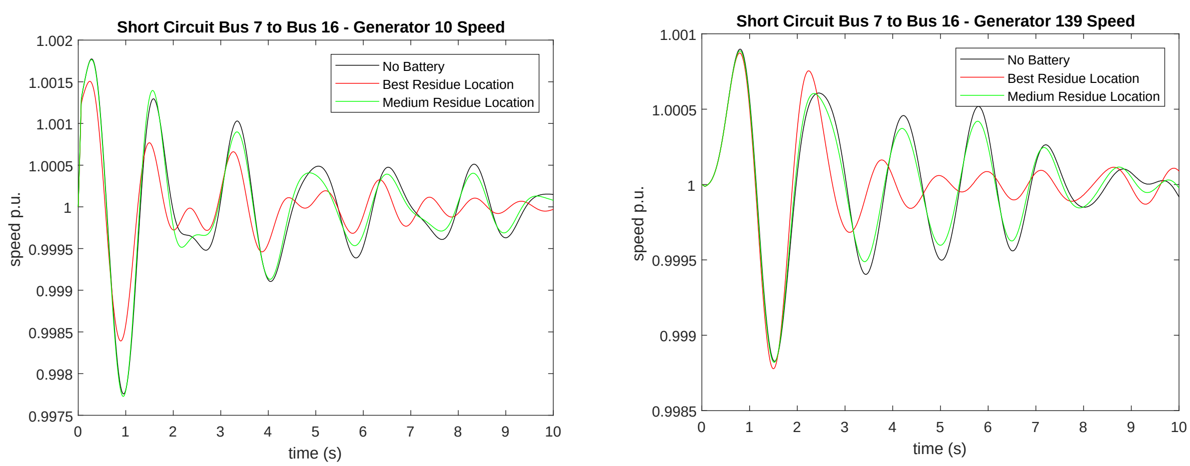

(a) Gen 10

(b) Gen 139

Figure 2.6: Short circuit for line 7 to 16 for mode with DR 9.730%. Simulations show speeds for (a) Generator 10 and (b) Generator 139 for various energy storage system

areas through a set of lines to the west and the south. With a high amount of power flowing out to the west and the power flowing in from the south to this area, causes the area to oscillate with Northern California. This type of low frequency, inter-area oscillation requires regulation devices to help dampen out the oscillating machines before damage occurs. Now that the key areas have been identified for the current WECC system and the RSI index is applicable to a large power system with multiple inter-area modes, there is a need to identify the impact of regulation resources and oscillations and how the key areas change with wind penetration levels up to 30% in the following chapters.

Table 2.3: Residue data and damping ratio of critical inter-area modes in the WECC Decommission Scenario

Mode Number	Mode	DR	RSI	Bus with Max Residue
1	-0.190+5.629i	3.373	0.000497	161
2	-0.198+4.783i	4.138	0.000742	139
3	-0.207+4.649i	4.445	0.000416	139
4	-0.307+6.375i	4.806	0.001166	3
5	-0.298+5.635i	5.275	0.002618	161
6	-0.362+3.707i	9.730	0.0029028	10

Chapter 3

Primary Frequency Control with Wind Turbines

As the WECC system moves towards higher renewable penetration levels, the penetration level will be increased by (a) addition of new non-conventional generation and (b) the decommission of conventional power plants. When the system inertia is reduced from the incorporation of wind power plants the ROCOF of the power system will be increased for disturbances seen by the grid [22]. Primary frequency control is handled by the governors of the generators which will automatically adjust the power output of the machines in response to a frequency excursion caused by an event such as a generator outage to maintain frequency stability. In the case of such an event, the speed of the synchronous generators will slow down and convert the kinetic energy into active power in response to the frequency deviation [23]. The location of the frequency controller for frequency excursions is not relevant because frequency is a system wide phenomena [9]. Similar frequency capabilities can be implemented with WTGs. The wind turbine will use either an inertia emulator acting through the active power controller or a deloaded-operation by pitching the blades of the wind turbine [24]. In this study, the wind turbine model will consider an inertia emulator control scheme. The inertia emulation scheme will adjust the rotor torque to adjust the power output. This can be seen where an increase in torque causes the rotor to slow down, and the wind turbine then runs at above rated power to improve the frequency response of the system [25].

Not only can frequency controllers help improve the system response during a frequency excursion, but they can also be used to help the oscillations in the system. This leads to the idea of finding the locations with the best impact for the frequency excursion and the system oscillations. If the WTGs are used for damping oscillations, there is a phenomenon where during an oscillation the power and torque follow oscillating trajectories. This means there will be oscillating forces at the shaft which will affect the speed of the drive train. This mechanical behavior can potentially increase the wear and tear and potentially reduce the overall lifespan of the wind turbine. From this behavior, wind turbine owners may be less willing to implement primary frequency control due to the increased potential damage to their wind farms. The goal is to improve system stability through the use of frequency control from the wind farms to assist with the damping of inter-area oscillations. A way to lessen and assess the risk of implementing frequency control is to assign a small portion of the wind turbines to participate in frequency control with the oscillations. If a system operator will implement the controllers, this reinforces the idea of finding the best location for the controllers out of the existing wind turbines to reduce the risk of damage and improve the stability of the system. The goal of this section is to analyze if the WTGs can participate in inertia emulation-based frequency control to help dampen the inter-area oscillations.

The model of the wind turbine used is a generic Type 3 wind turbine model as shown in the Figure 3.1. The Type 3 model is based on the doubly-fed induction generator (DFIG) for the wind turbine generator. The generic wind turbine control scheme includes both the mechanical and the electrical controls of a DFIG based upon the IEC Standard 61400-27-1 [26]. The mechanical portion of the control scheme use a pitch angle controller to control the pitch angle of the wind turbine blades, a turbine model to determine the wind power based upon the pitch angle, and a two mass model for the shaft which determines the output power of the turbine [26]. The electrical controls are used to regulate the reference speed and the voltage of the DFIG. The WTG model uses maximum power tracking to determine the reference speed by using a power reference, which is determined by both the speed controller and the over-frequency controller. The electrical controls consist of a set of measurements from the power grid, a PQ controller to determine the current based upon the active and reactive power references, a rotor current controller, and a compensation controller that will determine the voltage of the DFIG [26]. There is also a set of protection schemes to make sure the current and voltage limits are not violated. This allows for the analysis of the effectiveness of the RSI with a regulation device other than energy storage devices. The regulation device, implemented at the location based upon the RSI, is a complex wind controller that gives a detailed description of both the mechanical and electrical controls. This controller leads to a better understanding of the impact that wind turbines will have on the power grid. An adjustment made to the generic wind turbine model is the addition of a voltage controller to allow for better reactive power control and an inertia emulation-based frequency controller in place of the original over-frequency controller. The voltage controller uses the voltage difference of the terminal of the WTG and reference voltage to determine the reference Q. This Q reference is compared to a direct measurement from the WTG in the original model. The primary frequency controller, shown in Figure 3.2, uses the change in frequency to determine the change in the power output, but implements a washout filter to account for the high frequency changes. These changes are associated with events such as a step change or a generator outage. The washout filter allows for steady-state frequency values other than the rated frequency [27].

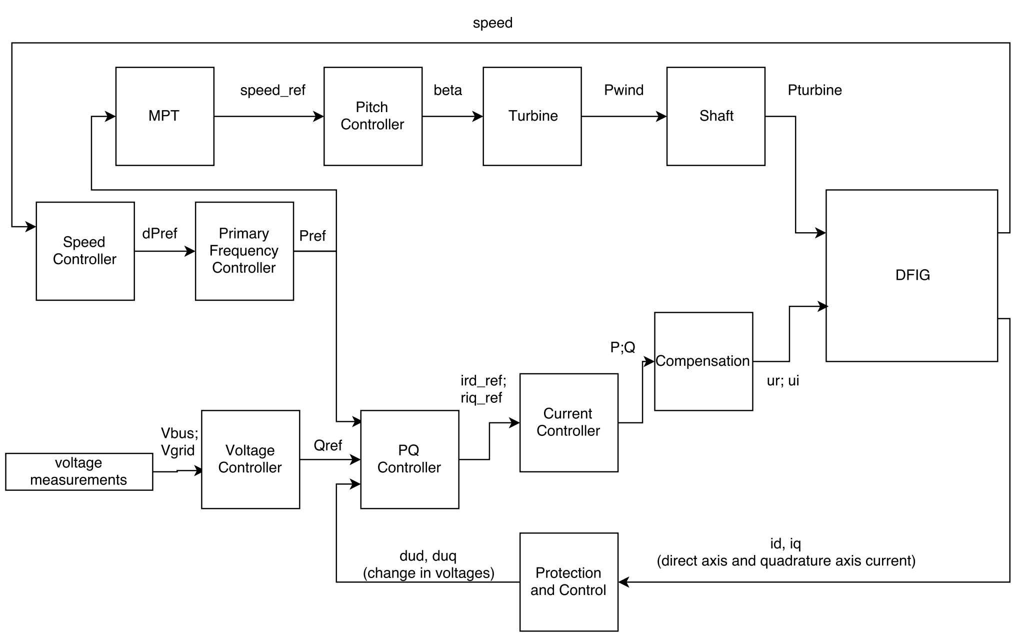

Figure 3.1: Type 3 Generic Wind Model Control Scheme

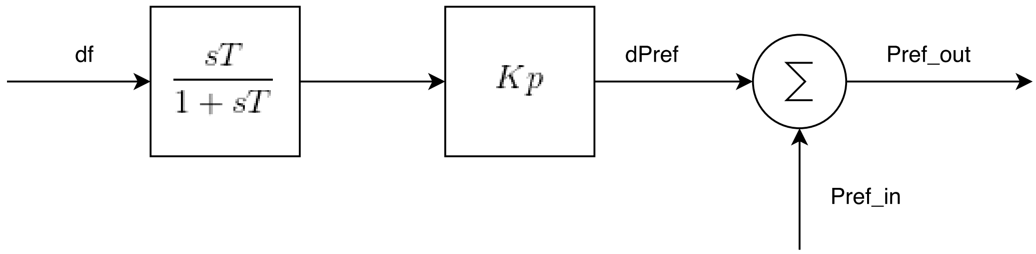

Figure 3.2: Frequency Control Scheme

3.1 Decommission Case

In order to study the effect of the frequency controller with the wind turbines, there needs to be an understanding of how the WTGs will affect the system. By looking at the damping ratios of the system's inter-area modes for scenarios 1-4 of Table 3.1, these values will give an idea of how the critical modes will change as the renewable penetration level increases. When looking at the damping ratios of the individual oscillations, there is not an overall consensus on how the modes will change. This is due to the changes of inertia in the WECC. These inertia changes are caused by the removal of generators, which have varying sizes of inertia. The removal of inertia will have different effects depending on how strongly the machine was involved in the oscillations for that area. In Scenario 2 (10% wind generation), lower inertia machines that are involved in critically damped modes are removed which increase the damping ratio. This is because the low-inertia machines are no longer swinging against the higher inertia machines. In Scenarios 3 and 4 (20% and 30% wind generation), the damping ratio of the modes change differently depending on the machines removed. The machines are higher inertia machines in high inertia areas, which have varying participation levels in the system oscillations. In order to understand how the WECC changes with wind power, the inter-area modes that occur in each scenario are studied, in particular, modes 1, 3, and 5 from Table 3.1.

The inter-area modes 1, 3, and 5 are chosen based upon the frequency and the mode shape pertaining to the oscillation. For a given oscillation, the residue index is studied to see how the location of the regulation devices change. The RSI slightly decreases in magnitude for the PQ buses as the wind penetration level increase as shown in Figure 3.3 for mode 5 with

Table 3.1: Damping ratio changes for varying wind penetration levels in %

Mode Number	Base Case	10% Wind	20% Wind	30% Wind
1	3.373	3.506	3.101	2.508
2	4.138	3.737	$N\backslash A$	$N\backslash A$
3	4.446	3.974	4.111	4.174
4	4.806	$N\backslash A$	$N\backslash A$	$N\backslash A$
5	5.275	6.211	6.336	6.373
6	9.730	$N\backslash A$	$N\backslash A$	$N\backslash A$

damping ratio 5.275%. This change occurs because the decommissioned generators with low inertia are replaced by converter-based WTGs that do not participate in the oscillation. The PV buses in Figure 3.3 are 10, 158, 161, 4, and 5 with bus 4 containing a WTG. Compared to the slight decrease in the RSI at most buses, buses 4, 5, and 10 see an increase in the RSI of the inter-area mode. Theses changes are from the removal of generators 3, 5, 8, and 17 which causes generator 10 to be the only synchronous generator in the region to heavily interact with the oscillations in the grid. The removal of generators leads to a decrease in the inertia for that area. This is reflected by the increase of the RSI for buses 4, 5, and 10 in Figure 3.3. Although only one mode is shown, a similar phenomenon occurs with the other modes. The RSI decreases in buses not directly related to the oscillating machines as the renewable penetration level increases for the decommission scenarios. The generators left active in the reduced inertia areas see an increase in the RSI. This increase is due to the lower inertia areas compared to the base scenario of the WECC system and the higher involvement of the generators during the oscillations.

As the wind turbines are implemented into the power grid and conventional generation is removed, the system becomes more susceptible to faults which could cause a higher ROCOF. In order to see if we can improve the system's response to disturbances, primary frequency controllers will be tested with the wind turbines. Since frequency is a system wide phenomenon, the placement of controller for a given wind turbine will improve the frequency stability of the system. The controllers can shorten the life span of wind turbines, so in order to reduce the risk, why not choose the best location? The goal is to identify a few key locations that can be used in order to improve the frequency response of the system using

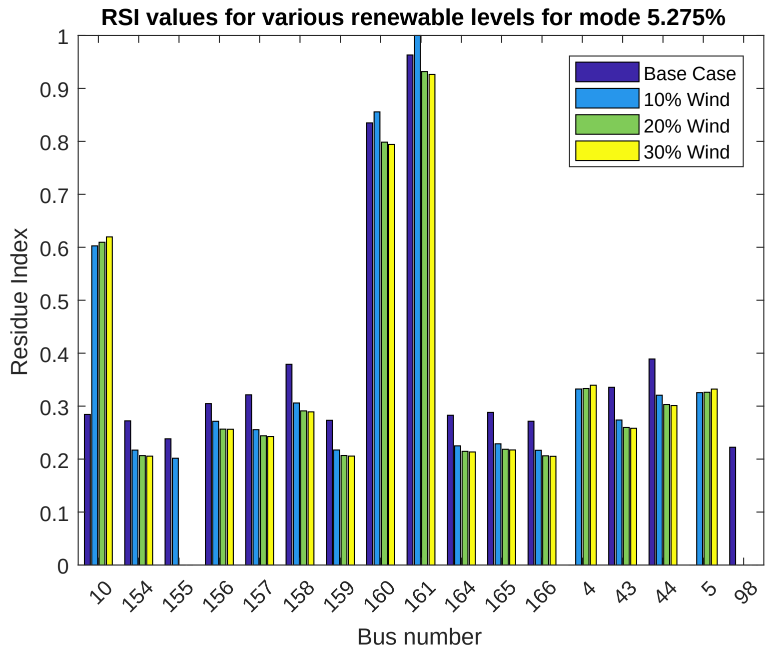

Figure 3.3: RSI for mode 5.275% for up to 30% wind

the wind turbine locations and the RSI. The RSI can be applied to identify the best locations for the primary frequency controllers in each wind scenario. For the inter-area oscillations of the base case scenario, the placement of the battery energy storage system was chosen for the maximum RSI value for a given oscillation. The location of the primary frequency controller is chosen based upon the best RSI limited to the WTG locations for all critically damped modes, which includes intra-area modes. The reason behind this is if a primary frequency controller is placed at a random wind turbine location with a low RSI this could lead to a minimal improvement towards the oscillation or even a negative impact, which could cause an increase in the magnitude of the oscillation. Each WTG turbine location has a different RSI value to the different modes. This means that there is not a single ideal location for the most improvement. What is possible is to look at the impact of each WTG to see the best impact on the eigenvalue sensitivity analysis, and tune the controllers to help impact the most sensitive modes. The highest RSI value for a single mode will be related to a specific wind turbine. Even though this may not directly affect all modes, there is an improvement in the system due to a more critical mode being damped. Given that there will be multiple wind farms in the grid and that each wind turbine will affect different modes, proper tuning of the frequency controllers will significantly improve the system.

As mentioned above, the primary frequency controllers are only related to a few buses in the entire system. This means the decision of which mode affected is determined by the mode most impacted by the frequency controllers, which may not be the overall maximum RSI. What can be done is for a given wind scenario, the highest RSI between WTG locations and all critical oscillations modes is identified. These values are identified in Table 3.2 which give the best RSI for the most impacted oscillation mode between the WTGs. As shown in Table 3.2, we can see WTG 4 has the highest RSI and the best relation to the mode 4.938%. This can be verified by looking at the eigenvalue plot for the various proportional gain values of KP for the primary frequency controller at WTG 4 in Figure 3.4. The figures shows the initial point is denoted by the black circle, and the different gain values are shown by the red x symbols. The figure clearly shows the eigenvalue λ = -0.206+j4.164 is the most sensitive to the proportional gain Kp. As Kp is increased the most sensitive mode moves towards the imaginary axis. This can be fixed by compensating the mode, but when attempting to compensate the most sensitive mode, there was an issue with the eigenvalue λ = -0.198+j5.639. Although the most sensitive mode was properly compensated to move away from the imaginary axis, the mode -0.198+j5.639 moves towards the imaginary axis causing the system to become unstable. The issue with this mode is related to generator 76 and is not able to be compensated through a device such as a power system stabilizer (PSS) due to the shape of the oscillation. The heavily participating generators in the oscillation are 76, 69, 139, and 29, which besides generator 76 are already tuned with a PSS. This makes the tuning of the PSS of generator 76 have little impact. This shows that a WTG not near the heavily participating machines for a given oscillation will have issues being used for frequency control. This would disqualify the other WTGs in Scenario 1 since they are not located near the heavily participating machines as well. This needs to be analyzed for higher wind penetrations to see if this remains true.

So now when looking at the different wind scenarios, the highest RSI values at each location are used to determine which modes are most sensitive to the WTGs. Table 3.3 shows which WTG has the highest residue, which mode that RSI value relates to, and what

Table 3.2: Best RSI and mode DR for Scenario 2 (10% wind generation)

Wind Turbine Location	Mode (DR)	RSI
2	4.938%	1.30e-3
4	4.938%	1.79e-3
7	4.938%	1.38e-4
16	4.938%	1.73e-4

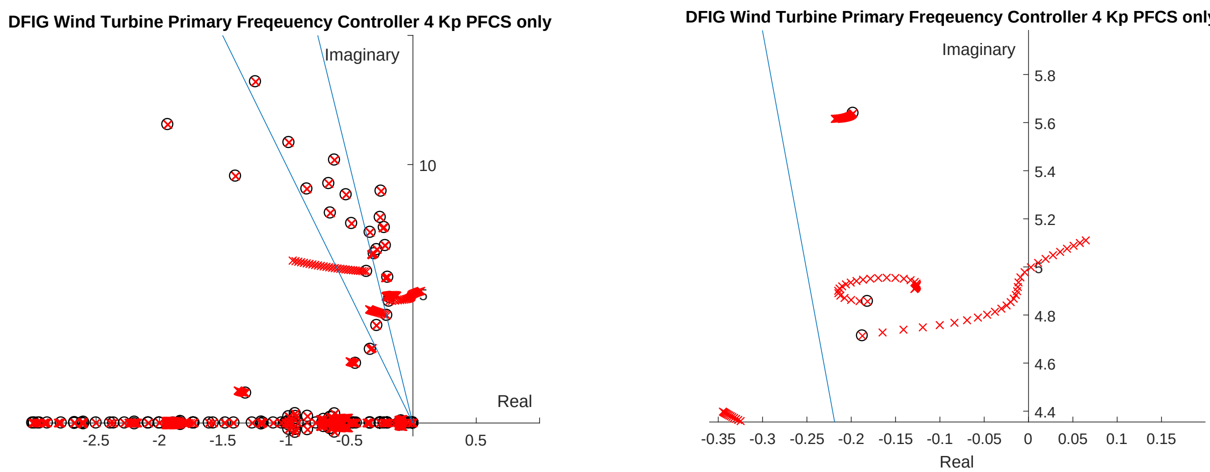

(a) WTG 4 **(b)** WTG 4 Zoom

Figure 3.4: (a) Eigenvalue plot for the primary frequency controller Kp values (b) zoom in on critical mode

machines are heavily participating in the oscillation. The heavily participating machines are defined because in Scenario 2 where although the highest RSI was at WTG 4, the machine nearby was generator 10 which is weakly related to the oscillation compared to the other generators. This leads to issues with trying to control the mode due to the heavily participating machines driving eigenvalues towards instability as shown in the eigenvalue sensitivity analysis shown in Figure 3.4. Scenarios 3 and 4 show similar issues with the mode $\omega = 5.6$ rad/s moving towards the imaginary axis for small Kp values as shown in Figure 3.5.

Table 3.3: Wind Turbines for highest RSI values for all wind scenarios

Scenario	WTG	RSI	Mode DR (%)	Heavily Participating Machines
2	4	1.790e-3	4.938	29, 76, 69, 78
3	146	3.159e-4	1.925	76, 29, 139
4	138	3.325e-4	1.653	76, 29, 139, 12, 14
5	156	3.263e-3	2.849	44, 161, 158
6	156	3.298e-3	2.900	161, 158, 44
7	156	3.242e-3	5.994	161, 158, 14

(a) WTG 146

(b) WTG 138

Figure 3.5: Eigenvalue plot for the primary frequency controller Kp values showing the sensitive modes (a) WTG 146 (b) WTG 138

3.2 Scale Wind Generation Case

Following the same idea as the decommission case, the scale wind generation case is studied in this section. First the critical inter-area modes are compared between wind penetration levels shown by Table 3.4. Table 3.4 shows how the damping ratios change as the renewable penetration level increases without the removal of any of the synchronous generators, which shows that the low damping (< 5%) modes become more critical. When looking at the DRs after the wind turbines are installed, the DR of the modes with DR greater than 4% have slightly increased. From 10% to 20% of renewable penetration level the majority of the modes increased in damping due to the larger generators being less stressed with the aid of power injection from the wind farms. From 20% to 30% of wind penetration level the DR is relatively the same, but there is a wind farm installed at bus 171 due to the wind power limits at the other wind farm sites.

In order to have an understanding of how the RSI will change with increasing renewable penetration, the RSI for mode 5 is studied in Table 3.4. Figure 3.6 shows the significant RSI values that are involved in the oscillation using an RSI value of 0.25 p.u. as a cutoff point for an easier comparison. This oscillation was between the generators 8, 35, 44, 158, and 161 (Group 1) and generators 5, 10, 111, and 117 (Group 2). For comparison, the system inertia is the individual generator inertia for that generator's power base in MVA converted to the system base of 100 MVA. The sum of the system inertia values of Group 1 is 279 s and the inertia value for Group 2 is 502 s. In the RSI plot, the highest RSI is related to the weaker inertia area of Group 1, and this RSI value increases as we move up in wind penetration levels. There is a phenomenon where generators 44 and 158 drop off from having significant values due to the sensitivity of the bus with respect to active power injection, but we see an increase with bus 156 and generator 5 for their RSI values. This is due to the loading in the respective generators compared to the generators' max MVA rating. The buses 156, 160, and 161 are connected along a single pathway, where there is high power injection to reach the load areas in the system. So as the wind penetration increases, the generation from buses 44, 158, and 161 decreases, and the generation from the WTG 156 increases, the lines are stressed further to deliver the power to the load. In this case, the generators 44 and 158 are less stressed in terms of their active power limits, while WTG 156 is more stressed and the RSI values of the buses around WTG 156 increase. Although generator 10 and 5 are not directly near a WTG, they have an increase in their RSI values. This is most likely due to the relationship between the generation and load where they have to import power into the area in order to meet the load demand, so the residue increases for the need of active power. This need for active power injection is reflected when the generators participate in an oscillation and need the extra power injection to help dampen out the oscillation.

Now that there is an idea of how the system will change with respect to higher wind penetration, the RSI shows that a few buses are key points with regards to determining the best location for regulation resources regarding active power control. This study will look at

Table 3.4: Damping ratio changes for varying wind penetration levels by percentages % for the scale generation scenario

Mode Number	Base Case	10% Wind	20% Wind	30% Wind
1	3.373	3.045	2.933	2.976
2	4.1383	3.289	3.454	3.494
3	4.446	5.067	4.856	4.895
4	4.806	5.401	6.085	6.101
5	5.275	5.679	6.024	5.994
6	9.73	9.104	8.709	8.589

how frequency control at WTGs can be applied to assure stability due to the change in the shape of the residue for Scenarios 5-7. Although there were limitations in the decommission cases (Scenarios 2-4) regarding the issue of the highest RSI being related to a set of machines that are a distance far away from the WTG, the scale case shows more promise with more WTG locations. Without the decommissioning of generators there is not a loss of oscillations between certain machines. With the placement of the WTGs spread more evenly, there is a higher chance of having an impact with the frequency controllers. This can be seen from Table 3.3 where the overall RSI values in Scenarios 5-7 are higher than the RSI values of Scenarios 2-4. The impact of the maximum RSI value at bus 156 can be assessed with the eigenvalue plot of WTG 156 for the different wind penetration levels in Figures 3.7 and 3.8. The figures show how the eigenvalues of the system are affected as Kp is increased. Due to the plots being stable, a comparison of the effects of the frequency controllers on the critical oscillations in the system can be performed.

Scenario 5 is first evaluated with the mode λ = -0.158+j4.810 with DR 3.289%. The mode is excited through a short circuit of line 154 to 164, where the goal is to improve the damping in the oscillation to help improve the system stability. Figure 3.9 shows the speed plots of generators 158 and 161 for the short circuit of line 154 to 164. The plot compares the effect of WTG 156 with and without frequency control for the 10% wind penetration. Similarly, Figure 3.10 show the response of the speed of the generators 158 and 161 for a short-circuit of line 156 to 160. The short-circuit excites the mode λ = -0.218+j7.504 with DR 2.900% for the 20% wind penetration level. For the 30% wind penetration level, Figure 3.11 shows the speed

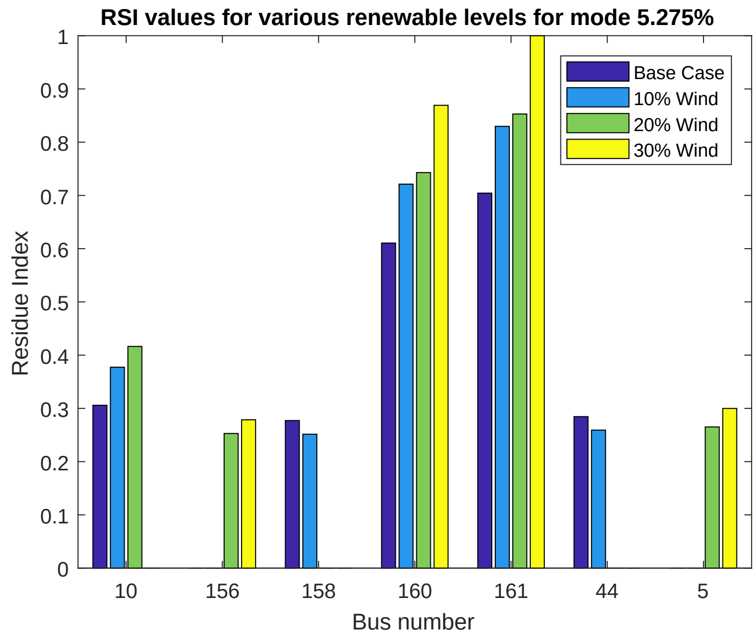

Figure 3.6: RSI for mode 5.275% for up to 30% wind

response for a short-circuit of line 156 to 160 excites the mode λ = -0.225+7.496i with DR 3.000%. The modes for the 20% and 30% are not related to the inter-area oscillations, but are the most sensitive modes. From each figure there is a negative impact on the oscillations. This may go against the idea of using the frequency controllers in specific WTGs to help with damping the inter-area oscillations, but the RSI can still be analyzed for the buses at the WTGs. The maximum RSI values from Table 3.3 are 3.263e-3, 3.298e-3, and 3.242e-3 for Scenarios 5-7. Although this is unfortunate that the wind controllers are unable to provide damping for the critical oscillations based upon the RSI, this shows that the RSI has a minimum value that will damp the mode. If a poor location is chosen, then the operator will only harm the system. The simulations show that when the WTGs participate in frequency control, there was not an improvement in the damping of the oscillations. This was due to two main factors. The first issue was that this is a multi-mode system which share a given pool of generators, whereas the analysis performed is to improve a single mode out of all the critically damped modes. The second issue is that the same generator can appear in many of these critically damped modes, which causes problems when compensating a given mode. The specific instance in the decommission scenario that appeared is using a PSS at

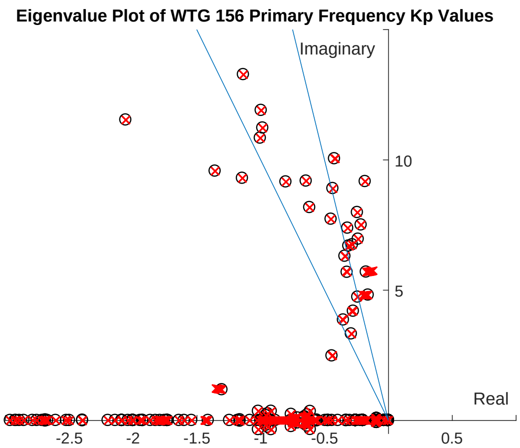

(a) WTG 156

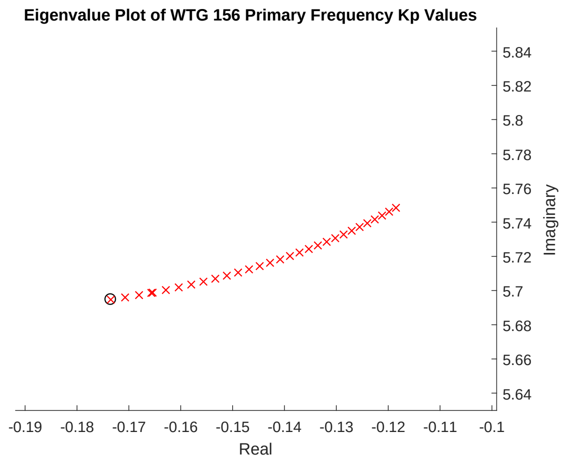

(b) WTG 156 Zoom

Figure 3.7: Eigenvalue plot for the primary frequency controller Kp values for WTG 156

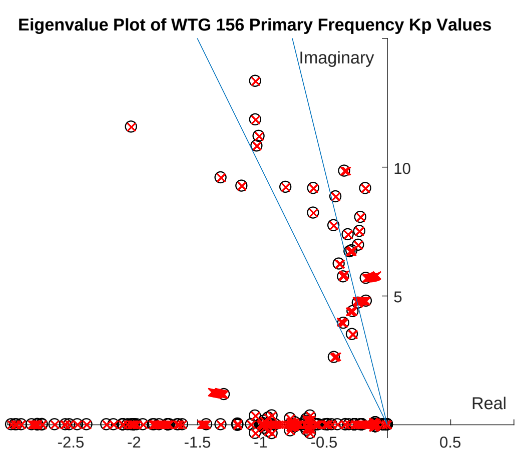

(a) WTG 156 for Scenario 6

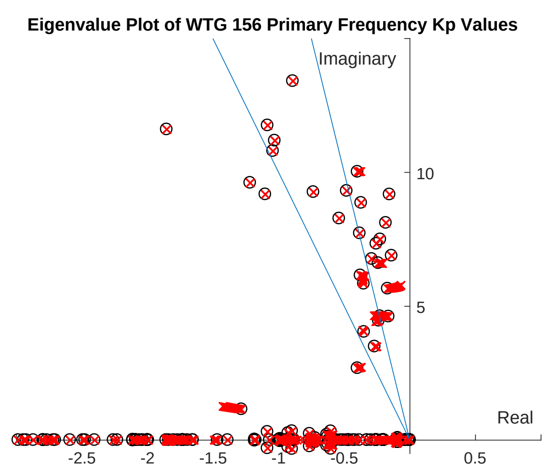

(b) WTG 156 for Scenario 7

Figure 3.8: Eigenvalue plot for the primary frequency controller Kp values showing the sensitive modes of WTG 156 for (a) 20% wind generation (b) 30% wind generation

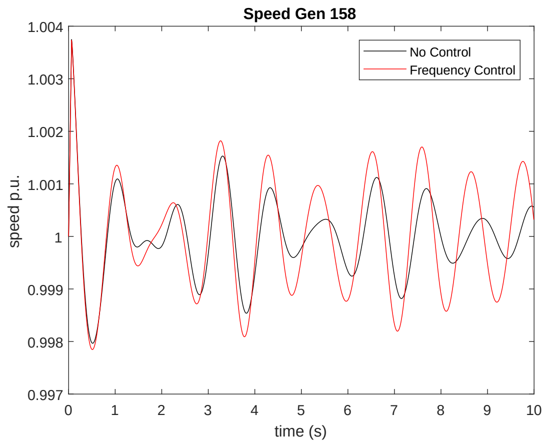

(a) Speed of Generator 158

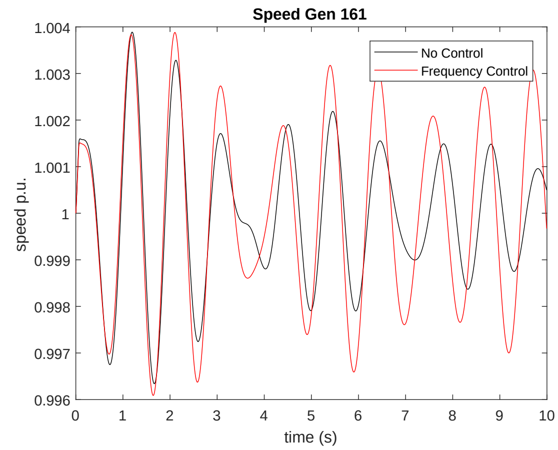

(b) Speed of Generator 161

Figure 3.9: Speed plots for a short-circuit event of line 154 to 164 for 10% wind generation

generator 76 to compensate the mode λ = -0.198+j5.639. The issue is the other generators in the north, near generator 76, all have compensation through PSS as well, which made any further compensation have little impact. A similar scenario appears for the scale generation cases. In short, there is a complication when compensating the actuators of the system due to the complexity of a multi-mode system. The frequency controller used has been shown to improve the frequency response in a test system, but the control scheme is directly involved with the oscillations in the system. This analysis shows that there was a negative impact when the controller interacts directly with the oscillations, so an idea is to use a controller that does not interact directly with the oscillations for future studies. One such scheme, shown by Lopez and Almeida, uses a pitch control, a static converter, and a deloaded power curve which adjusts the power reference of the WTG for frequency changes in the system [24]. This scheme was proven to work for a small system and could potentially be applied for larger test systems.

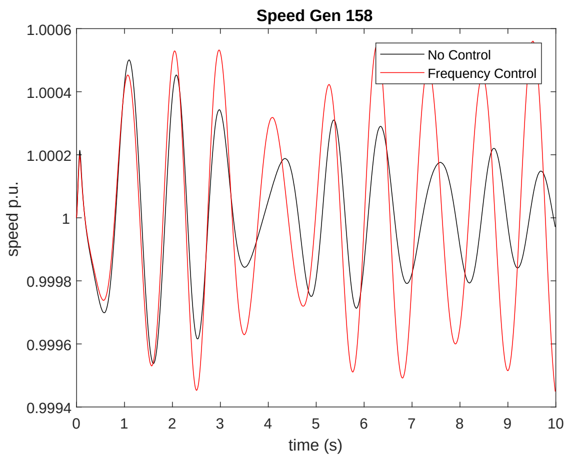

(a) Speed of Generator 158

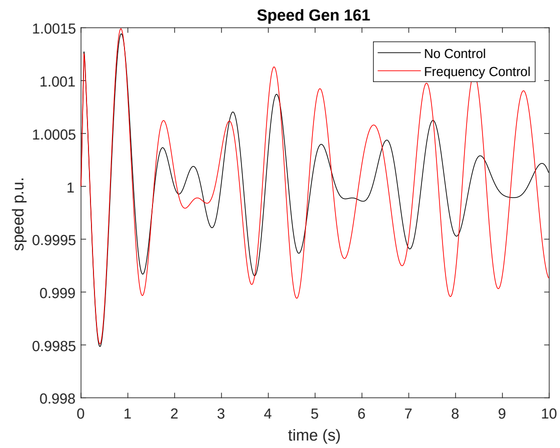

(b) Speed of Generator 161

Figure 3.10: Speed plots for a short-circuit event of line 156 to 160 for 20% wind generation

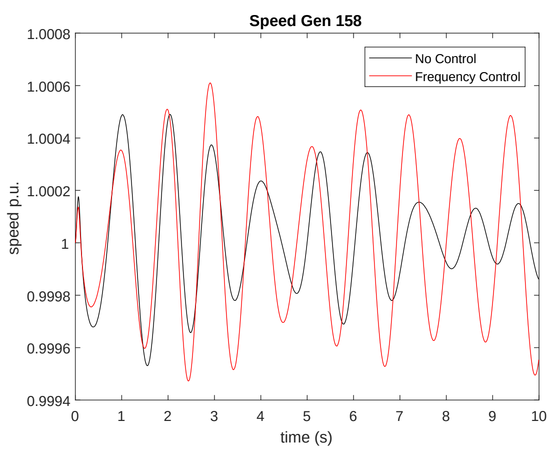

(a) Speed of Generator 158

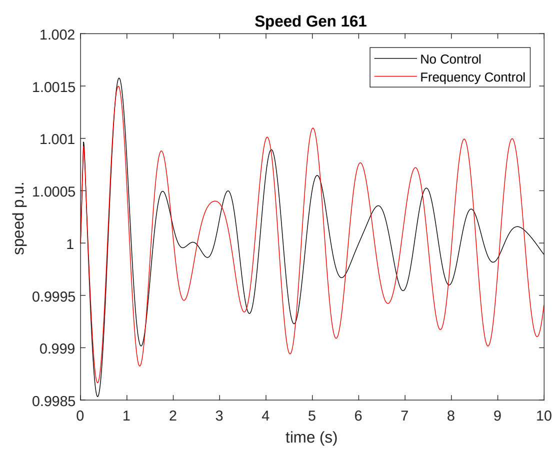

(b) Speed of Generator 161

Figure 3.11: Speed plots for a short-circuit event of line 156 to 160 for 30% wind generation

Chapter 4

Impact of Energy Storage Devices

In the last few chapters, the RSI was evaluated for the base case and the wind scenarios for the best placement of active power regulation through the BESS and the primary frequency control. For the proper placement of the control, the damping and response of the system is increased. In the base case, there was an overall improvement using the global maximum RSI value to choose the location of the regulation device. In the wind scenarios, the idea was to use the WTGs with a frequency controller to improve the critical oscillations related to a given WTG, but the results had shown that the RSI was too low and the WTGs had a negative impact on the system. In this part of the thesis, the impact of energy storage systems based upon the RSI towards the critical oscillations is analyzed.

4.1 Decommission Case

In the previous section, the critical modes were identified across all levels of wind penetration in Table 3.1. For the Decommission Scenarios only modes 1, 3, and 5 are shown to exist in all scenarios. These modes are studied to see how they change with higher wind penetration levels, where mode 5 with a DR of 5.275% was already analyzed in Figure 3.2 and shows a slight decrease in all buses with higher wind penetration. We want to verify this for each critically damped inter-area mode, so mode 1 and 3 are analyzed. These modes will show how the system changes for the critically damped inter-area modes.

Figure 4.1 shows the RSI for all the decommission scenarios regarding mode 1 with DR 3.373%. When looking at Figure 4.1, the biggest detail is that the 20% wind scenario has the highest residue in comparison to the other scenarios for the mode. The machines oscillating against each other are 158, 44, 161, 29, 117, 111, 115 (Group 3) against 78, 76, and 69 (Group 4). This high residue at the 20% wind scenario is that the actual RSI value index is about 10 times the size of the other scenarios. This can be seen where for the base case, 10% case, 20% case, and 30% case the RSI values are 4.97e-4, 5.36e-4, 4.44e-3, and 4.723e-4 respectively. This would explain why the the bar plot has the sudden spike in the 20% wind scenario. The maximum RSI values occur in the buses 44, 158, 161, and 111 because these are a part of the weaker inertia group of generators. In this group, the smallest inertia generator has an inertia value of H_{161} = 25 s and the largest inertia generator has a value of H_{111} = 87.8 s. Generator 161 is a high residue point in the 20% scenario, where the generator is one of the only three synchronous generators left in the eastern area of the WECC system with the other two being generators 158 and 44. Generator 161 has the lowest inertia out of the generators. The reason why the 30% case drops in the inertia value is most likely because there is a generator decommissioned in the northern node, which is one of the heavier synchronous generators participating in the critical oscillation. This would lessen the magnitude of the oscillation involved due to the lowered amount of kinetic energy exchanged and the change in the shape of the oscillation.

Next we want to analyze mode 3 with a DR of 4.446%, where Figure 4.2 shows the RSI across all decommission scenarios. This plot follows more closely what was seen in Figure 3.2 where there is a decrease in the residue index across most buses as the system moves up in wind penetration. Unlike before in Figure 4.1 where the 20% scenario has the highest residue, the 20% does not have high RSI values with this mode. In the previous mode 1 there was a participation with the weak inertia generators 161, 158, and 44, which do not appear in mode 3. The generators in mode 3 are higher inertia generators in the system with the lowest being $H_{10} = 73.5$ s. The inertia of the two participating generator groups are H_{Group3} = 940 s and H_{Group4} = 860 s, where the highest RSI value is seen at generator 10. This is due to generator 10 being not only the smallest inertia generator, but also having a location far away from the other generators. Generator 10 is the only generator in the east that is

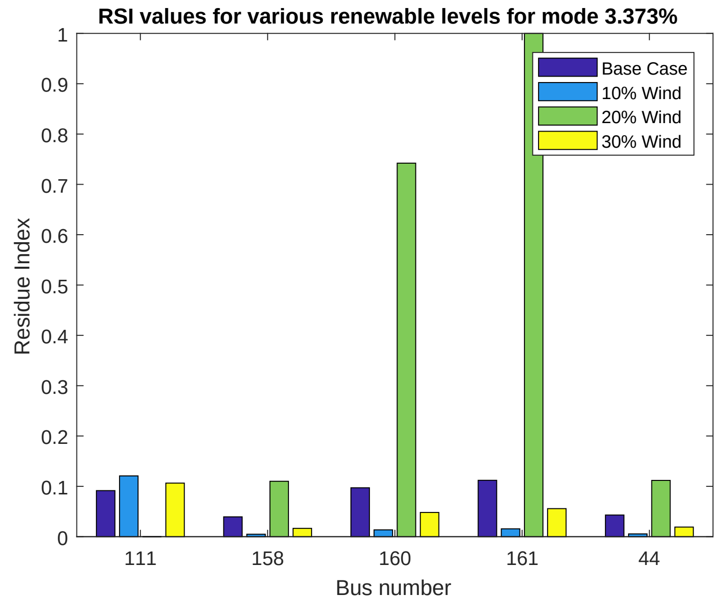

Figure 4.1: RSI for mode 1 with DR 3.373% for up to 30% wind

involved in the oscillation. When the inertias of the machines are not skewed to one specific oscillating generator group and location, then the RSI shows a decrease for the majority of the system. The weaker inertia generator group and the surrounding area do see a slight increase.

Now that the RSI values have been shown for the three critical modes, the RSI needs to be evaluated between wind scenarios in order to verify the findings. From our analysis of the wind turbine frequency controller in Chapter 3, there needs to be a minimum RSI value for the regulation device to have a positive impact. As shown in Table 4.1, the modes have differing RSI values for the maximum location. In the previous chapter, the impact of the controllers had little effect with the given magnitude of the RSI. In this study, the mode that is more susceptible to the placement of the BESS will be mode 5 due to the magnitude of the RSI being 10 times larger than the other two modes. Mode 5 will be studied to verify the changes in the time domain simulations following the RSI. Although mode 1 and mode 3 are not studied with time domain simulations due to the low magnitude of the RSI, the transformation of the RSI in critical areas are still important as previously discussed.

From Table 4.1, the maximum RSI value is listed across the different wind scenarios for mode 5 with DR 5.275%. The oscillation will have $\omega = 5.635$ rad/s with the higher

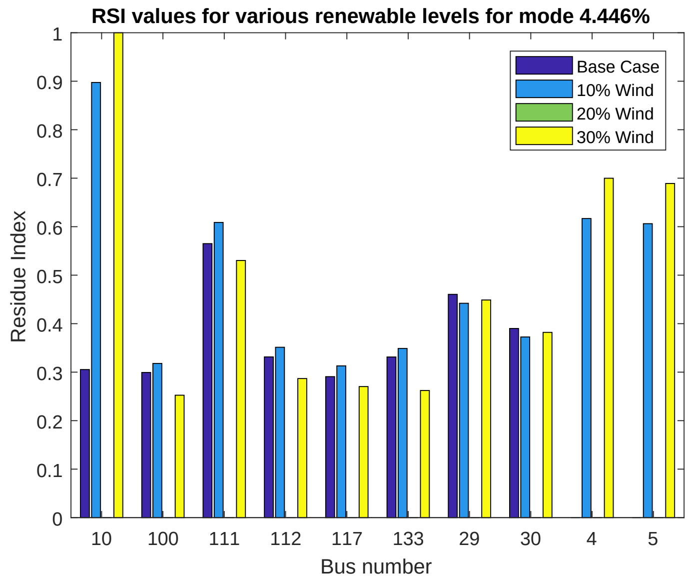

Figure 4.2: RSI for mode 3 with DR 4.446% for up to 30% wind

Table 4.1: RSI comparison between critical modes for all decommission scenarios.

Mode	DR (%)	Base (0%)	10%	20%	30%
1	3.373	4.97e-4	5.36e-4	4.44e-3	4.72e-4
3	4.446	4.16e-4	6.06e-4	5.13e-4	6.75e-4
5	5.275	2.60e-3	2.72e-3	2.53e-3	2.52e-3

participating machines being 161, 158, 10, and 117. Due to the BESS impacting the machines in the oscillation with a similar effect, only generators 161 and 158 that have the more significant responses are shown. In Figure 4.3, the time domain simulations show the comparison of the speed responses of the high participating generators 161 and 158 with and without the BESS. The fault that occurs is a load step of 2000 MW at bus 4 that excites mode 5. The BESS is placed in the maximum RSI with respect to each wind penetration. In Chapter 2, the effect of the BESS with the RSI was already shown between the maximum and other significant RSI valued locations, so in Figure 4.3 only the best RSI valued location is shown.

As we can see from Figure 4.3, the BESS has a positive impact on the time domain simulations. As we move up in wind penetration we can see that the system oscillations reflect the weakened system inertia. For the same disturbance of a 2000 MW load step at

Figure 4.3: Speed plots with and without BESS for mode 5 with DR 5.275% for all decommission scenarios

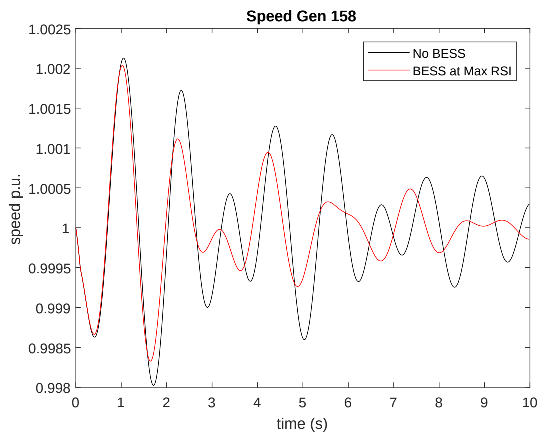

(a) Base - Speed of Generator 158

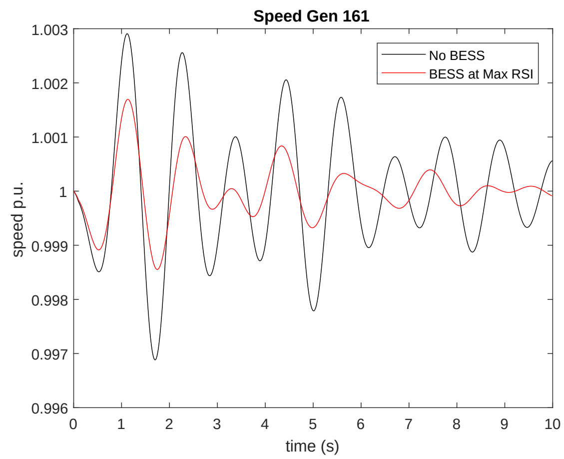

(b) Base - Speed of Generator 161

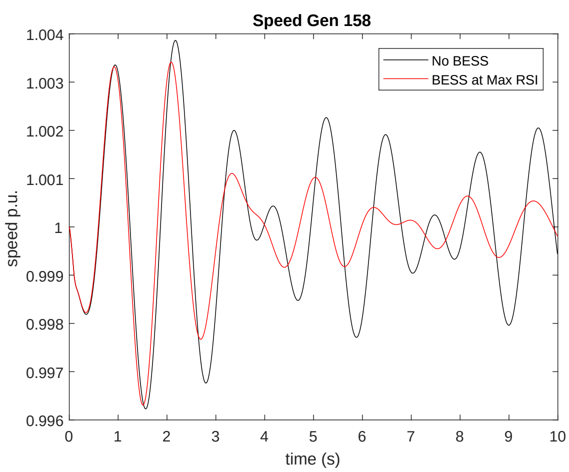

(c) 10% Wind - Speed of Generator 158

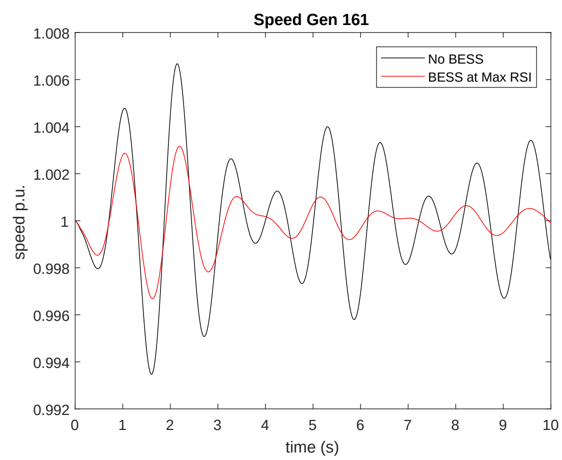

(d) 10% Wind - Speed of Generator 161

Figure 4.3 continued

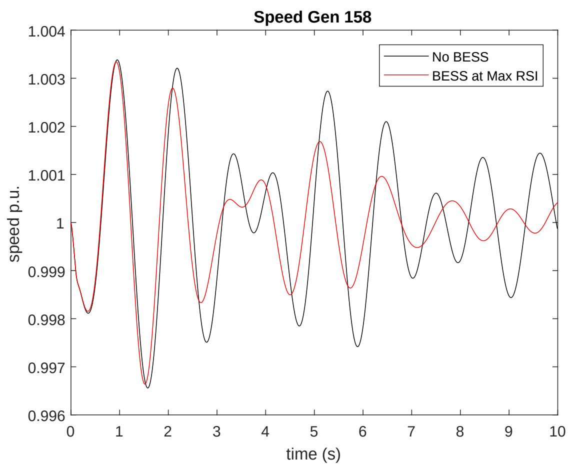

(e) 20% Wind - Speed of Generator 158

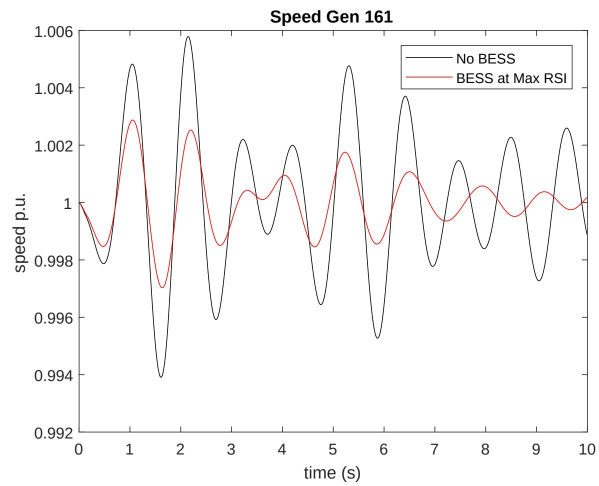

(f) 20% Wind - Speed of Generator 161

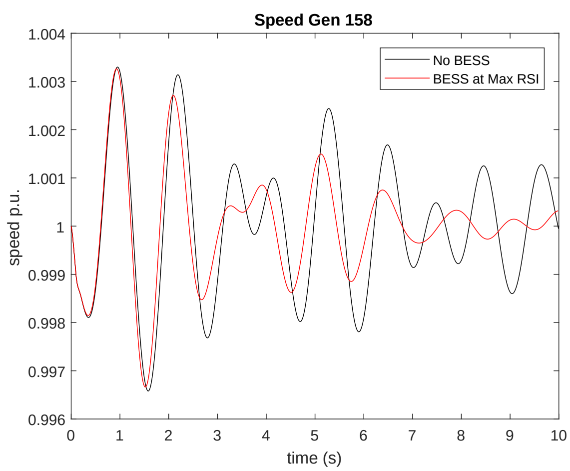

(g) 30% Wind - Speed of Generator 158

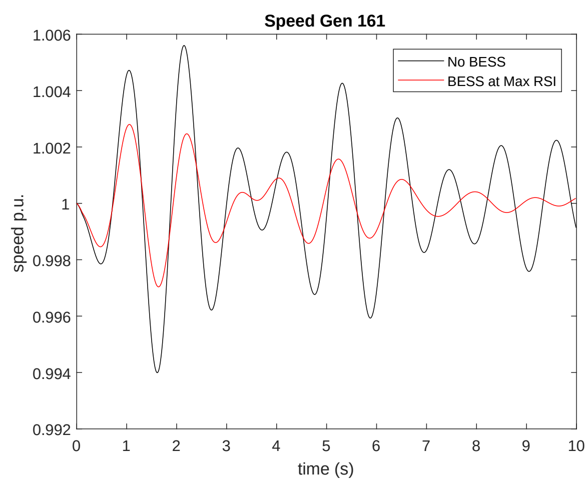

(h) 30% Wind - Speed of Generator 161

Figure 4.3 continued

bus 4, there is a minor change in the magnitude of the oscillations. As seen in Figure 4.3a, the base case has a max speed value of 1.002 p.u. and a minimum speed value of 0.998 p.u., whereas the system with 30% wind penetration has a max speed value of approximately 1.003 p.u. and a minimum speed value of around 0.997 p.u. Although the order of the magnitude for the oscillation is small (1e-3), there is a clear point where the disturbance is damped. This occurs around 6 seconds for the base scenario and moves towards being damped around 7 seconds for the system with higher levels of wind generation. This verifies the RSI matches what Figure 3.2 shows, where the RSI lowers as the system increase the amount of wind generation.

So now that the RSI has been analyzed for a few key modes, how do the maximum RSI values change between all scenarios for every critical mode? This is referring to if bus A has 1 maximum RSI out of all the critical modes for the base scenario, meaning that bus is the best location to place the regulating device to damp a critical mode A. Does the number of maximum RSI values increase for higher levels of wind generation such as bus A would now have a higher number of maximum RSI across all critical modes? An example of this is bus A has the maximum potential to dampen mode A in the base case compared to bus A being able to damped modes A, B, and C at 30% wind with a regulation device. The change in maximum RSI values is related to a bus shows the areas that require more active power support to help improve the system stability for a given oscillation as the wind penetration level increases.

Figure 4.4 shows the number of maximum RSI values for the critical modes at a given bus. The values in the figure are integers that represent the number of critical modes that are most sensitive to a regulation device placed at the corresponding bus. This means for bus 161 has the highest residue values for 3 different critical modes. This location is one of the weaker inertia machines and generator 161 is involved in both intra-area and inter-area modes. As the system moves up in wind penetration there is an increase in Figure 4.4 for buses 10, 111, 39, 42, 44, 64, and 161. This means that these locations will affect more modes as the wind penetration level increases if the BESS is located here. These locations are near the areas where generators have been decommissioned. This shows that the areas are more susceptible to active power injection since the areas no longer have as

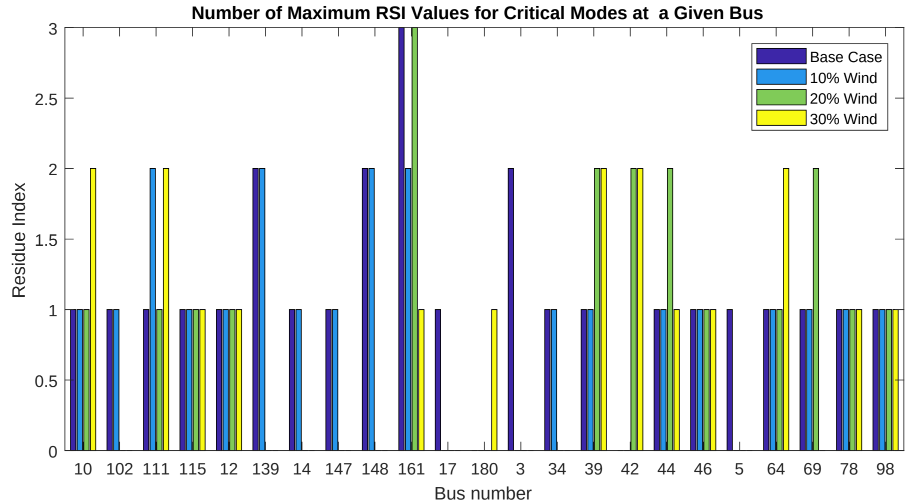

Figure 4.4: Number of maximum RSI values across all critical damped modes for the Decommission Scenarios

much capability to withstand an oscillation due to the lowered inertia. Specifically, the generators 39 and 42 in Southern California become more sensitive due to the installed WTGs in the south that affect the powerflow in the region. The figure shows as the system move towards higher renewable penetrations, the low inertia generators in load centers end up having a higher number of residue values. These generators are: 10, 17, 39, 42, 44, 148, and 161. The highest residue values occur near generators that will need extra support due to higher stresses from the limited number of synchronous generators and lowered inertia. The changes in the decommission scenarios occur due to the constant topology changes between wind penetration levels, where the lower inertia generators and generators in areas of power imbalance are the ones that see the highest number of residue increases in relation to the critical modes.

4.2 Scale Wind Generation Case

Previously analyzed is the decommission case where SGs are replaced with WTGs concerning the impact on critical eigenvalues. Here a scenario of how the WECC would change if all SGs are left active and WTGs are added to the power grid is analyzed. In this study case, the SGs have their power generation scaled down to allow for the installment of wind generation.

Table 4.2: RSI comparison between critical modes for all scale wind generation scenarios.

Mode	DR (%)	Base	10%	20%	30%
1	3.373	4.97e-4	4.37e-4	4.84e-4	5.37e-4
2	4.143	7.59e-4	2.787e-4	3.82e-4	4.86e-4
3	4.445	4.16e-4	6.71e-4	6.05e-4	5.79e-4
4	4.806	1.17e-3	1.41e-3	1.66e-3	2.04e-3
5	5.275	2.62e-3	3.08e-3	3.17e-3	3.72e-3
6	9.73	2.90e-3	2.34e-3	1.91e-3	1.70e-3

This means for the 10% scenario, all SGs are scaled down to 90% power generation of the original output and the installed wind turbines inject power to match that 10% difference. When looking at the active power injection for the different wind scenarios, Table 4.2 refers to the RSI values of the critical inter-area modes (less than 10% DR) for all scale wind generation scenarios. One major characteristic between the study cases is that the RSI has greater changes in value whenever there is a topology change in the system. Examples of this are when the wind turbines installed in the 10% wind case and the 30% wind case are shown in Table 4.2 In order to analyze the differences between the decommission case and the scale wind generation case, the changes in the RSI need to be compared, between the critical inter-area modes. Mode 1 with DR 3.373% and mode 3 with DR 4.446% are analyzed and the RSI of mode 5 with DR 5.275% is verified with time domain simulations. In Figure 4.5a, the RSI for mode 1 is shown for all wind levels. Since the decommission case has already shown the modes 1 and 3, the goal here is to understand how these modes change with the scale wind generation case. The mode 1 with DR 3.373% follows the previous findings of the scale wind generation case, where the residue slowly decreases with an increase in wind generation and a decrease in SG power output. There are no significant values for the 30% case which shows that residue has decreased except for a spike at the residue of bus 69. This is due to a topology change with the placement of a WTG at bus 171 which is near where the northern WECC and British Columbia connect to the rest of the WECC. The reason for the high RSI in bus 69 is the generator is now producing a fraction of the total rated power and has a smaller inertia compared to the other generators in the north. This causes the generator to require more support for the oscillation. Unlike the decommission case, the RSI

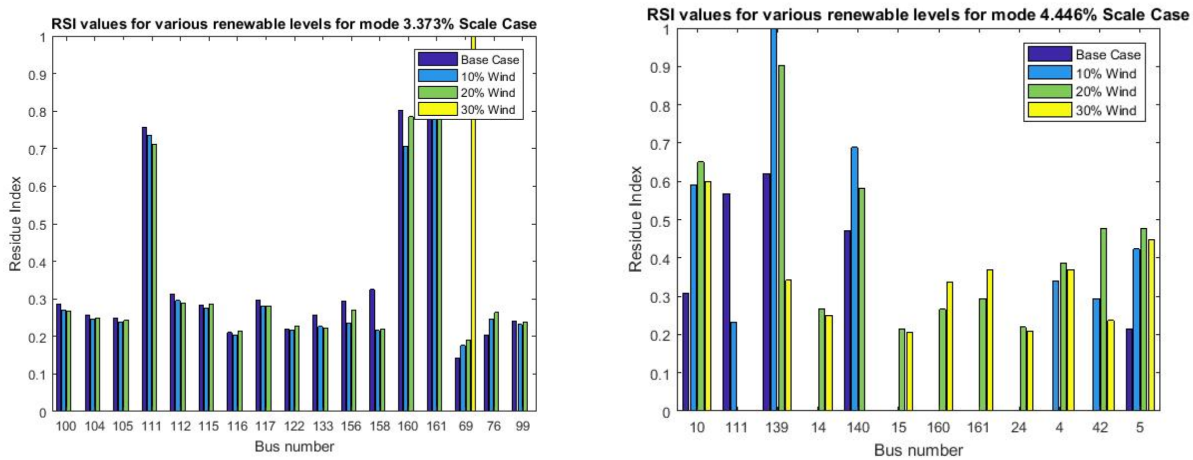

(a) RSI for mode 3.373% for up to 30%

(b) RSI for mode 4.446% for up to 30%

Figure 4.5: RSI plots for the modes with DR 3.373% and 4.446% for the Scale case

of the scale wind generation case changes in a gradual fashion due to the minimal changes in the topology of the system.

The RSI of mode 3 with DR 4.446% in Figure 4.5b shows the changes are different across the areas of the grid. Buses 139 and 140 are in the south of the WECC where there is a large increase in the RSI when wind generation is installed, but decreases as the wind penetration level increases. For the south-eastern area of the grid, represented by buses 4, 5, and 10, there is an increase in the RSI up to the 20% wind penetration level and for the eastern area, represented by bus 160 and 161, there is an increase up until the 30% wind penetration level. This shows that the south and the east part of the WECC system becomes more susceptible to changes in the active power and could require more support with the scale wind generation case. This can also be seen in the decommission case where buses 4, 5, and 10 have an increase in their RSI values. Figure 4.5 shows a quick summary of these results. Figure 4.5a shows the buses of the west have a decrease in the RSI and Figure 4.5b shows an increase of the buses in the south and east, which represents the buses that are more sensitive to support from the BESS.

Now that the modes 1 and 3 have been compared to the decommission case, the RSI of mode 5 needs to be verified for the time domain simulations with the load step of 2000 MW. When looking at Figure 4.6 there is a damping effect, but the damping occurs slower than in the decommission case. The effects of the BESS on generator 158 has a lower impact.

Figure 4.6: Speed plots with and without BESS for mode 5 with DR 5.275% for all scale wind generation scenarios

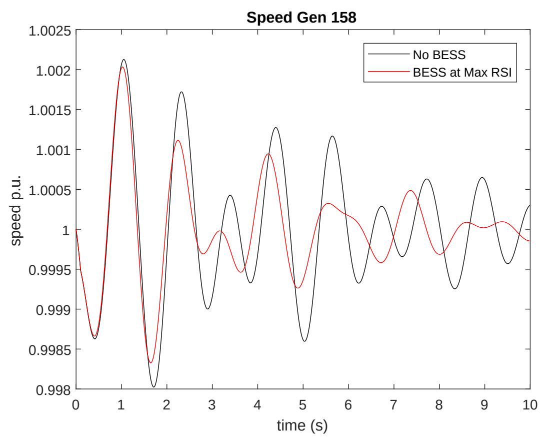

(a) Base - Speed of Generator 158

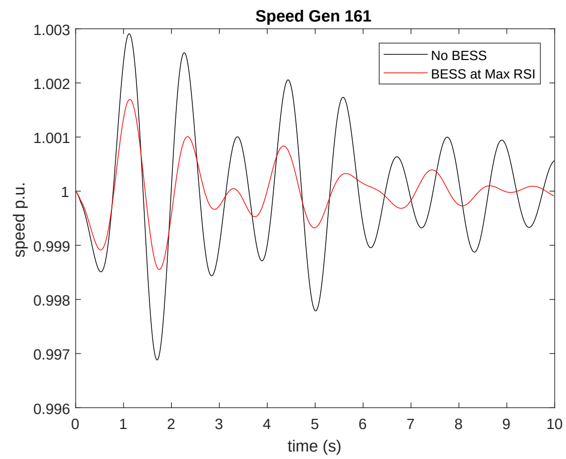

(b) Base - Speed of Generator 161

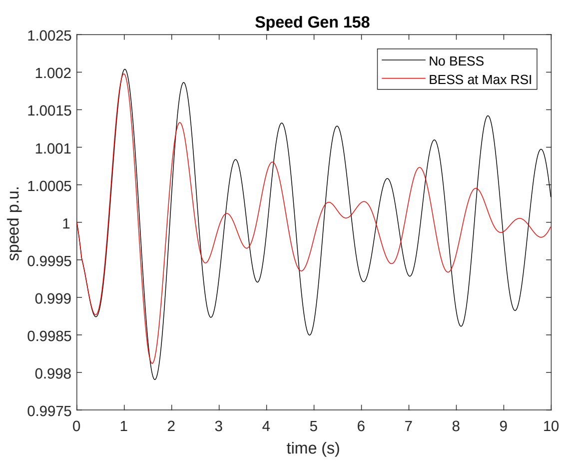

(c) 10% Wind - Speed of Generator 158

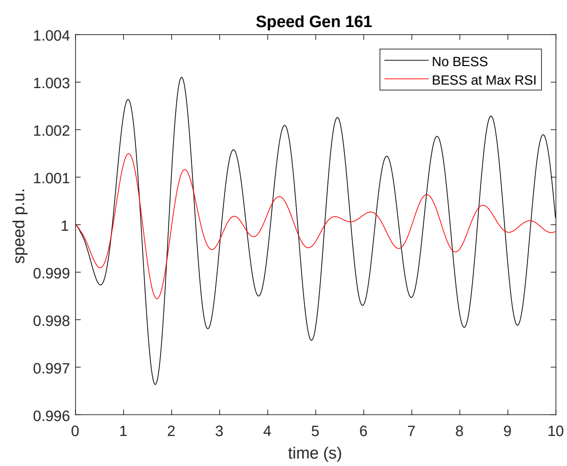

(d) 10% Wind - Speed of Generator 161

Figure 4.6 continued

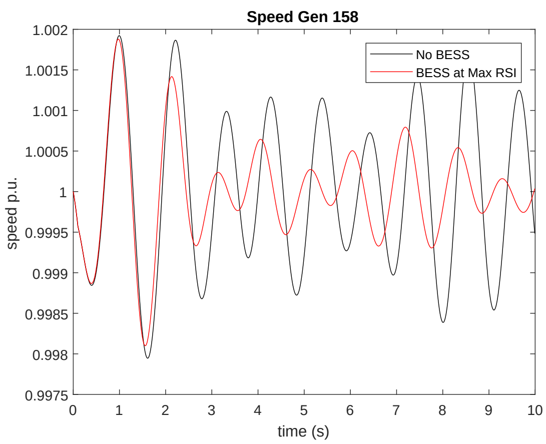

(e) 20% Wind - Speed of Generator 158

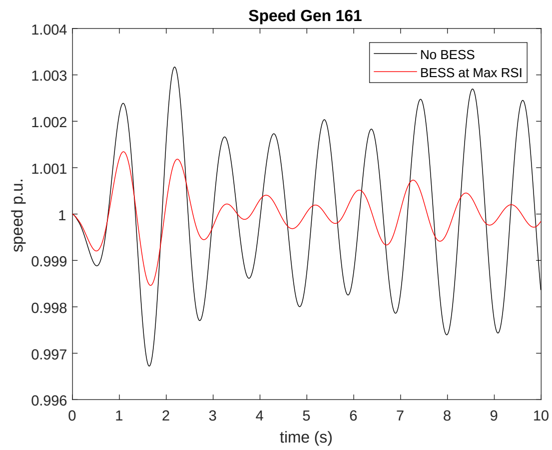

(f) 20% Wind - Speed of Generator 161

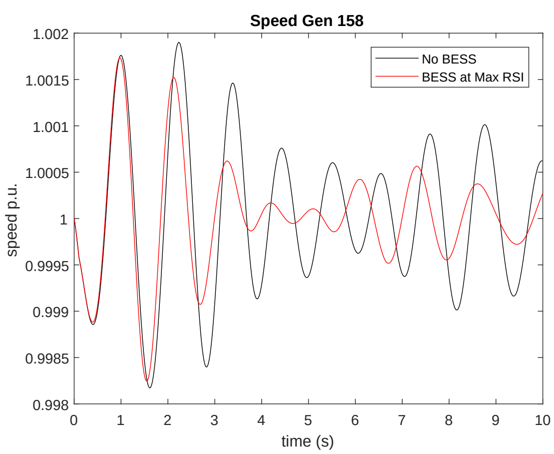

(g) 30% Wind - Speed of Generator 158

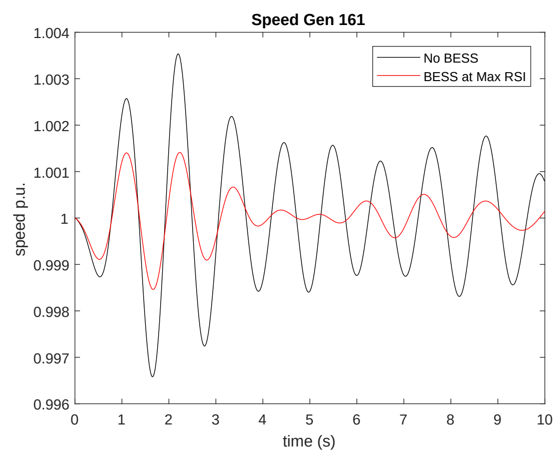

(h) 30% Wind - Speed of Generator 161

Figure 4.6 continued

The magnitude of the speed still has a noticeable deviation from 1 p.u., but the system has a faster time response around 5 seconds in each scenario. Although the response is faster, the implementation of the BESS does not completely dampen the oscillation. For generator 161, there oscillation is damped around 3 seconds for each wind level. In the scale wind generation cases, the magnitude of the oscillation is not as high only being between 0.997 p.u. to 1.004 p.u. for generator 161 and between 0.9985 p.u. to 1.002 p.u. for generator 158. In the decommission case, the magnitude of the speeds for generator 161 is between 0.994 p.u. to 1.006 p.u. and the magnitude for the speed for generator 158 is between 0.997 p.u. to 1.003 p.u. Not only do the time domain simulations show that the RSI is working for the scale wind generation case, but also verifies that the decommission case is more susceptible to the oscillation due to the lowered inertia of the system. This is not an issue for the oscillation shown, but for larger events there could be damage to the system without proper support for the weaker areas of the system.

Once again, the changes between the number of maximum RSI values at the buses for all critical modes needs to be analyzed. This tracks which buses will impact a number of critical modes, reflected by the number of maximum RSI values. In Figure 4.7, we see that the majority of buses do not change their number of maximum RSI. This shows that although these buses are more susceptible to active power injection for an oscillation, they are not the most vulnerable areas across the wind penetration levels. From the changes in the plot, the highest difference in the locations will be between the base system to the 10% wind penetration level. This is due to the addition of wind turbines which change the topology of the system. From the 10% to 20% wind penetration level, there is no change to the topology. There is a change in system operation where the power of the generators is scaled down and the generation of the WTGs is increased. There is a change in bus 69, due to the reduction of power at generator 69 and the addition of WTG 171 from the 20% to 30% wind penetration level. Generator 42 has an increased number of RSI maxima, which is from the reduced power output of the generator. The power output was already low (325MW) compared to the rest of the system. The RSI changes show that there is more power being imported to make up for the difference in generation and load in the south-west of the WECC. The areas with the highest impact to multiple oscillations will be bus 161 and bus 42. These buses

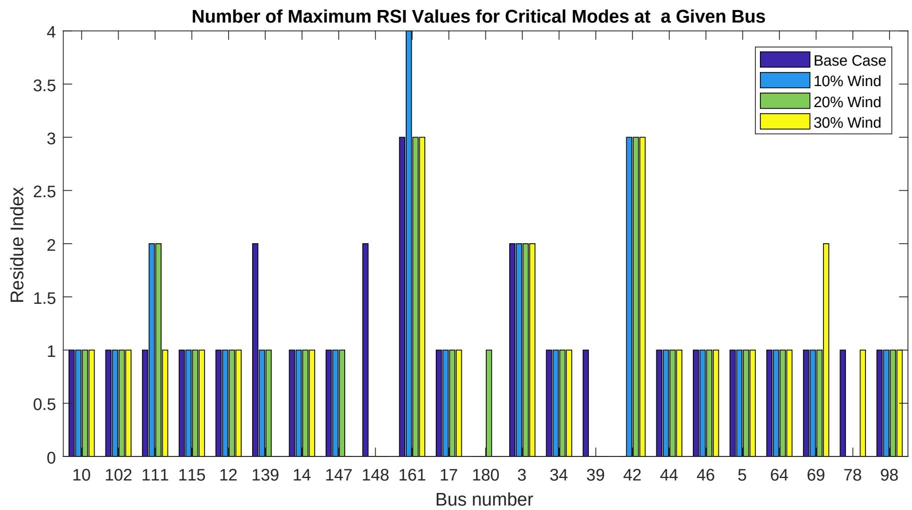

Figure 4.7: Number of maximum RSI values across all critical damped modes for the Scale Scenarios

were identified in the decommission case as well, which shows that the southwest and the east are areas of interest to help improve the response of the system regarding the critical modes. To summarize, when looking at the scale wind generation scenarios, the system will not have major changes in the RSI once the WTGs have been implemented. The largest change to the RSI is due to the topology changes in the grid and not the operation of the grid, although the operation needs to be stable in order for the RSI to be accurate.

Chapter 5

Conclusions

From the time-domain simulations, there are a few key points in the system where the application of an energy storage system will have a significant effect. The simulations have shown there exists a minimum RSI value for the WECC system to be around the order of 1e-3 for the BESS to have a significant effect towards an oscillation. As the wind penetration increases, the thought of using frequency control with wind farms to participate in the oscillations was not feasible due to the multi-mode phenomena and the inability to compensate the most critical modes. The RSI indicate areas sensitive for active power injection through regulation resources. As the WECC moves toward higher renewable penetrations, the southeast and southwest are susceptible to changes in the grid due to the low inertia machines and the distance away from other generation sources. In either study case, generator 161 is one of the most active generators that participate in the critical oscillations. There needs to be extra support in this area to help improve the system stability to certain oscillations. Generator 161 is in a region far away from the other areas of the system, which can lead to an oscillation that severely damages the local participating machines nearby. Lastly, the main differences seen for the RSI of the system is when topology changes occur, otherwise there were no major changes in the critical areas with only operational changes in the grid.

Future work will include the analysis of the WECC system with higher renewable penetrations up to 80% renewable generation. This analysis will look into more of the relationship between the RSI and the system characteristics to help give a guideline on how to place regulation resources for power systems. The wind turbine frequency control will be pursued with a different controller that is not highly involved with oscillations such as those controllers based on a de-loaded operation. This will potentially help the issues of compensation for the actuators in the WTGs and the complexity of the multi-mode systems. The application of the residue will be applied for reactive power control to see if the index can be applied for identifying reactive power regulation device locations in the WECC. The goal is to improve the understanding of how complex power systems change with higher renewable energy penetrations.

Bibliography

[1] G. Energy, "Western wind and solar integration study," tech. rep., NREL/SR-550-47434. Golden, Colorado: National Renewable Energy Laboratory, 2010. vii, 1, 12

[2] WECC, "2016 state of the interconnection," tech. rep., Salt Lake City, Utah:Western Electricity Coordinating Council, 2016. 1

[3] D. Zografos and M. Ghandhari, "Estimation of power system inertia," in *Power and Energy Society General Meeting (PESGM), 2016*, pp. 1–5, IEEE, 2016. 1

[4] A. Ulbig, T. S. Borsche, and G. Andersson, "Impact of low rotational inertia on power system stability and operation," *IFAC Proceedings Volumes*, vol. 47, no. 3, pp. 7290–7297, 2014. 2

[5] S. Santoso and M. Singh, "Dynamic models for wind turbines and wind power plants," *NREL (National Renewable Energy Laboratory). Austin, Texas*, 2011. 2

[6] J. Quintero, V. Vittal, G. T. Heydt, and H. Zhang, "The impact of increased penetration of converter control-based generators on power system modes of oscillation," *IEEE Transactions on Power Systems*, vol. 29, no. 5, pp. 2248–2256, 2014. 2, 3

[7] S. B. Karanki and D. Xu, "Optimal capacity and placement of battery energy storage systems for integrating renewable energy sources in distribution system," in *Power Systems Conference (NPSC), 2016 National*, pp. 1–6, IEEE, 2016. 3

[8] Y. Liu, S. You, and Y. Liu, "Study of wind and pv frequency control in us power grids—ei and ti case studies," *IEEE Power and Energy Technology Systems Journal*, vol. 4, no. 3, pp. 65–73, 2017. 3

[9] H. Silva-Saravia, H. Pulgar-Painemal, and J. M. Mauricio, "Flywheel energy storage model, control and location for improving stability: The chilean case," *IEEE Transactions on Power Systems*, vol. 32, no. 4, pp. 3111–3119, 2017. 3, 4, 13, 19

[10] M. E. Raoufat, K. Tomsovic, and S. M. Djouadi, "Dynamic control allocation for damping of inter-area oscillations," *IEEE Transactions on Power Systems*, 2017. 4

[11] N. J. B. Prabha Kundur and M. G. Lauby. 4, 5, 10

[12] G. Rogers, "Modal analysis of power systems," *Power System Oscillations*, pp. 31–73, 2000. 5

[13] H. Pulgar-Painemal, Y. Wang, and H. Silva-Saravia, "On inertia distribution, inter-area oscillations and location of electronically-interfaced resources," *IEEE Transactions on Power Systems*, 2017. 6, 13

[14] F. L. Pagola, I. J. Perez-Arriaga, and G. C. Verghese, "On sensitivities, residues and participations: applications to oscillatory stability analysis and control," *IEEE Transactions on Power Systems*, vol. 4, no. 1, pp. 278–285, 1989. 6

[15] D. Trudnowski and J. Undrill, "The minniwecc system model," *Oscillation damping controls*, 2008. 6, 8

[16] S. Maslennikov, B. Wang, Q. Zhang, E. Litvinov, *et al.*, "A test cases library for methods locating the sources of sustained oscillations," in *Power and Energy Society General Meeting (PESGM), 2016*, pp. 1–5, IEEE, 2016. 6, 8

[17] P. Dandeno, P. Kundur, S. Umans, I. Kamwa, H. Karmaker, S. Salon, M. Shah, and A. El-Serafi, "Ieee guide for synchronous generator modeling practices and applications in power system stability analyses," *IEEE Std. 1110–2002*, pp. 1–72, 2003. 8

[18] W. J. S. I. Subcommittee, "Modes of inter-area power oscillations in western interconnection," tech. rep., Salt Lake City, Utah:Western Electricity Coordinating Council, 2013. 10

[19] R. Cresap and J. Hauer, "Emergence of a new swing mode in the western power system," *IEEE Transactions on Power Apparatus and Systems*, no. 4, pp. 2037–2045, 1981. 10

[20] R. Elliott, R. Byrne, A. Ellis, and L. Grant, "Impact of increased photovoltaic generation on inter-area oscillations in the western north american power system," in *PES General Meeting— Conference & Exposition, 2014 IEEE*, pp. 1–5, IEEE, 2014. 10

[21] IEC, "Short-circuit currents in d.c. auxiliary installations in power plants and substations, part 1: Calculation of short-circuit currents," 1997. 13

[22] G. Lalor, A. Mullane, and M. O'Malley, "Frequency control and wind turbine technologies," *IEEE Transactions on power systems*, vol. 20, no. 4, pp. 1905–1913, 2005. 19

[23] Y. G. Rebours, D. S. Kirschen, M. Trotignon, and S. Rossignol, "A survey of frequency and voltage control ancillary services—part i: Technical features," *IEEE Transactions on power systems*, vol. 22, no. 1, pp. 350–357, 2007. 19

[24] R. G. De Almeida and J. P. Lopes, "Participation of doubly fed induction wind generators in system frequency regulation," *IEEE transactions on power systems*, vol. 22, no. 3, pp. 944–950, 2007. 19, 32

[25] J. Aho, A. Buckspan, J. Laks, P. Fleming, Y. Jeong, F. Dunne, M. Churchfield, L. Pao, and K. Johnson, "A tutorial of wind turbine control for supporting grid frequency through active power control," in *American Control Conference (ACC), 2012*, pp. 3120–3131, IEEE, 2012. 19

[26] P. Sørensen, J. Fortmann, F. Jiménez Buendía, J. Bech, A. Morales, and C. Ivanov, "Final draft international standard iec 61400-27-1. electrical simulation models of wind turbines," in *Proceedings of the 13th International Workshop on Large Scale Integration of Wind Power and on Transmission Networks for Offshore Wind Power Plants, Berlin, Germany*, vol. 1113, p. 5, 2014. 20, 21

[27] H. Pulgar-Painemal and R. Galvez-Cubillos, "Wind farms participation in frequency regulation and its impact on power system damping," in *PowerTech (POWERTECH), 2013 IEEE Grenoble*, pp. 1–4, IEEE, 2013. 21

Vita

Michael Breuhl was born in San Diego, California on June 12, 1994. He received his Bachelor's Degree in Electrical Engineering from the University of Tennessee while doing undergraduate research in power systems. With the guidance of Dr. Hector Pulgar and support from his parents and family, he decided to pursue his Master's degree in Electrical Engineering in 2016. He defended his master's thesis in Fall 2017.